PREDICTION OF FREE SHEAR FLOWS

A COMPARISON OF THE PERFORMANCE OF SIX TURBULENCE MODELS

By B. E. Launder, A. Morse, W. Rodi,
and D. B. Spalding
Imperial College of Science and Technology

SYMBOLS

C_s	constant prefixing diffusion term in $\overline{uv}k\epsilon$ and $\overline{u_iu_j}\epsilon$ models
C_ϵ	constant prefixing diffusion term in ϵ equation
$C_{\epsilon 1}, C_{\epsilon 2}$	constants appearing in transport equation for ϵ
C_μ	viscosity constant
$C_{\phi 1}$	constant appearing in first part of pressure-strain simulation
$C_{\phi 2}$	constant appearing in second part of pressure-strain simulation
D	diameter of jet or of wake-generating body
D_i	diameter of inner nozzle
D_o	diameter of outer nozzle
D_{ij}	net diffusion flux of $\overline{u_iu_j}$
g	a function of $\overline{P/\epsilon}$ (see table 4)
h	specific enthalpy of fluid
k	turbulence energy, $\left(\overline{u^2} + \overline{v^2} + \overline{w^2}\right)/2$
l	length scale of turbulence
l_m	mixing length

M	Mach number
m	mass fraction of chemical species
P	production rate of turbulence energy
P_{ij}	production rate of Reynolds stress $\overline{u_i u_j}$
r	radial coordinate
r_o	radius of nozzle exit
$\tilde{T}$	stagnation temperature
$\tilde{T}_o$	stagnation temperature at nozzle exit
t	time
U	mean velocity in streamwise direction
U_e	velocity of free stream
ΔU	change in mean velocity across shear flow
U_i, U_j	mean velocity components
U_{min}	minimum velocity
U_o	initial (uniform) value of streamwise mean velocity
u,v,w	fluctuating velocities in x,y,z directions
$\overline{uv}$	kinematic shear stress
$\overline{u_i u_j}$	kinematic Reynolds stresses
x	coordinate in streamwise direction
x_i, x_j	general Cartesian coordinates

y coordinate in cross-stream direction

y_G effective width of shear flow

y_1, y_2 values of y at which effective internal and external edges of the shear flow occur

y^j coordinate in cross-stream direction where j is 0 for plane flows and is 1 for axisymmetric flows

α normalized mass fraction

δ_{ij} Kronecker delta

ϵ turbulence energy dissipation rate

θ momentum deficit (or excess) thickness of wake (or jet)

λ constant in mixing length model

λ_s proportionality constant relating length scale ℓ to y_G in k model of turbulence

μ_t effective turbulent viscosity

ρ density

σ reciprocal of spreading rate of mixing layer

σ_o value of σ when one stream is at rest

σ_ϕ effective turbulent Prandtl/Schmidt number (where subscript ϕ stands for h, k, m, or ϵ and denotes the diffused quantity)

Φ_{ij} pressure strain term in equation for $\overline{u_i u_j}$

Subscripts:

$\mathfrak{L}$ value prevailing along center line of a symmetric flow

E external boundary of shear flow

I internal boundary of shear flow

1 high-velocity edge of shear layer

2 low-velocity edge of shear layer

Bar over symbol indicates time average of turbulence correlation.

THE TURBULENCE MODELS CONSIDERED

The authors' work for the NASA Conference on Free Shear Flows has led to the exploration of the performance of three distinct classes of turbulence model. These classes are

(1) turbulent-viscosity models [1] in which the length scale of turbulence is found by way of algebraic formulas

(2) turbulent-viscosity models in which the length scale of turbulence is found from a partial differential equation of transport

(3) models in which the shear stress itself is the dependent variable of a partial differential conservation equation

In the context of the group's work on this subject, these classes might equally be, respectively, labeled "yesterday's" models, "today's" models, and "tomorrow's" models. At the time of the AFOSR-IFP-Stanford Conference in 1968, detailed exploration had been confined to models of class (1). In the intervening years, the development and application of models of class (2) has commanded the major part of the group's attention and, although models of class (3) have been in use since 1969, they have not yet been refined sufficiently to achieve the level of universality of which they are believed to be capable.

Two models have been examined in each class; thus, six different models have been tested. A complete mathematical statement of these models is provided in tables 1 to 6; a brief commentary on the models now follows.

Tables 1 and 2 detail the group's versions of two of Prandtl's turbulence models (refs. 1 and 2), namely, his 1925 mixing-length hypothesis $(m\ell h)$ and his 1945 turbulence

[1] A turbulent-viscosity model is one in which the shear stress is taken to be proportional to the local gradient of time-average velocity. The proportionality factor may vary from point to point in the flow and is usually calculated by reference to local turbulence quantities. It is not implied that the effective viscosity of the fluid is uniform across the mixing region.

kinetic energy model (k). For each model, the length scale is taken as proportional to the width of the shear flow although a different constant of proportionality is adopted for plane and axisymmetric flows. Table 1 reveals how the width of flow is defined.

The models of class (2), described in tables 3 and 4, employ a differential equation for the decay rate of turbulence energy ϵ as well as one for the turbulence energy. By introduction of this second turbulence transport equation, the need to prescribe the length scale is removed. The same two turbulence variables have been used in similar models by Harlow and Nakayama (ref. 3) and by Jones and Launder (ref. 4); other models having just two differential equations have also been used and described by Rodi and Spalding (ref. 5), Ng and Spalding (ref. 6), and Spalding (ref. 7). In the $k\epsilon 1$ model set out in table 3, the viscosity constant C_μ differs according to whether the flow is plane or axisymmetric. The more elaborate $k\epsilon 2$ model, detailed in table 4, has been adapted from that presented by Rodi (ref. 8). Rodi found that C_μ did not, in fact, assume a constant value but varied significantly with the distortion rate of the turbulence; the local rate of turbulence production divided by the rate of dissipation may be taken as a dimensionless measure of this quantity. Figure 1 shows Rodi's proposal for the dependence of C_μ on the ratio of production to dissipation at any station; the same variation is adopted in the $k\epsilon 2$ model.

In the two-equation class, attention has been confined to models employing k and ϵ as variables because extensive research at Imperial College has shown that, for free turbulent flows, the models of references 5, 6, and 7 produce almost identical results. Indeed, it can be shown that the identity is exact whenever the length scale of turbulence is uniform across the mixing region, and this condition is very nearly fulfilled for all free shear flows. Further, ϵ is preferable to the second variables of the other models when walls are present, for the $k\epsilon$ model alone can dispense with a wall-effect correction of the empirical constants.

The models set out in tables 5 and 6 are ones which do not involve the effective-viscosity concept. Table 5 presents the model of Hanjalić and Launder (ref. 9), which has been applied by its originators to predict a number of boundary layers and free shear flows. Besides the differential equations for k and ϵ, it embodies one for the kinematic shear stress $\overline{uv}$ as well. Lastly, model 6 presented in table 6 is an orthodox Reynolds stress closure of the kind first proposed by Rotta (ref. 10); it provides transport equations for all the Reynolds stresses $\overline{u_i u_j}$ and for the energy dissipation rate. If the turbulence Reynolds number is assumed high enough for the dissipative motions to be isotropic, only two processes remain to be simulated in the Reynolds stress equations: those of diffusional transport and of energy redistribution, the latter arising from correlations between fluctuating pressures and instantaneous velocity gradients. Two approximations have been explored for the first process and three for the second. In the flows

considered for this conference, only four of the Reynolds stresses are nonzero; the model thus entails the solution of five transport equations for turbulence quantities.

DETAILS CONCERNING THE PREDICTIONS

Method of Solving the Equations

The systems of differential and auxiliary equations governing the development of the mean and turbulent flow field have been solved by means of the finite-difference procedure of Patankar and Spalding (ref. 11). The main features of the method – that is, the use of normalized stream function as cross-stream independent variable and the employment of a grid-control system to fit the width of the grid to that of the shear flow – are perhaps sufficiently well known not to require further elaboration here. For the readers who are unfamiliar with the procedure, reference 11 documents the method in full and provides a listing of the basic computer program, GENMIX, from which codes used in the present work have been adapted.

The number of cross-stream nodes employed has varied from 20 to 40 according to the complexity of the initial profiles; grid nodes have been concentrated in regions where velocity gradients were steepest. A Control Data 6600 computer system was used. Typically, with 25 cross-stream nodes, the programs executed 70 forward steps per second for calculations employing the mixing-length hypothesis, where differential equations were solved for the mean-flow field (x-momentum, species, and stagnation enthalpy); with the Reynolds stress turbulence model and with the same number of nodes, about 35 forward steps per second were taken for isothermal, single-species flows. This number could certainly have been increased substantially, for to save human time many redundant instructions were not removed. No attempt has been made to include the influence of normal-stress gradients in the mean momentum equation since, for the turbulent-viscosity models, retention of these terms would render the equations elliptic in character. Likewise, corresponding terms in the turbulence equations have been neglected.

Initial Profiles

For all models except the mixing-length hypothesis, the initial profiles supplied by the conference organizers were insufficient to prescribe fully the starting conditions. Therefore, some of the profiles of the turbulence energy, of the Reynolds stress, and of the energy-dissipation rate had always to be estimated. This section explains the group's practices for generating the profiles.

(1) When the initial shear-stress profile was not supplied, a number of trial calculations were made based on a constant effective viscosity. The value of the constant was adjusted until the predicted development in the vicinity of the starting point agreed with the measured; this value of the effective turbulent viscosity was then used to determine

the initial shear-stress profile from the given velocity profile. The values adopted for each test case are given in table 7; they have been normalized by the product of the density ρ, the velocity change across the shear flow ΔU, and the diameter of the jet (or the diameter of the obstacle giving rise to the wake) D. In some cases the local value of density has been used, in others the values prevailing in the external stream; the third column of the table contains 1 or e as appropriate to identify the practice.

(2) Where the initial turbulence energy was not available, it was estimated from the shear-stress profile (either measured or determined as in practice (1)) by use of the following relation:

$$k = \frac{|\overline{uv}|}{0.3}$$

Close to an axis of symmetry, this formula gives an unrealistically low value of energy; in this region the k profiles are adjusted to apparently reasonable values based on turbulence data of other similar flows.

(3) In none of the test cases is the profile of energy dissipation rate directly available. It is calculated by inverting the viscosity formula

$$\epsilon = \frac{C_\mu \rho k^2}{\mu_t}$$

where μ_t is taken as the value of effective viscosity found in practice (1) or, when shear-stress data are available, is calculated from

$$\mu_t = - \frac{\overline{uv}}{\partial U / \partial y}$$

(4) For the $k\epsilon 2$ model, the initial value of the function $g(\overline{P/\epsilon})$ must be specified. For this inquiry, the usual practice has been to take this ratio as unity; however, for two of the wakes values greater than 1 have been assumed, and for two mixing layers values less than unity have been adopted. These test cases are identified in the fourth column of table 7.

DISCUSSION OF THE PREDICTIONS

Preliminary Remarks

Predictions have been made with the four models of classes (1) and (2) of all the 24 test flows except test case 24. The last of the flows was omitted from this inquiry because over much of its development the flow appeared not to be fully turbulent and because these models have not yet been adapted to the prediction of low Reynolds num-

ber phenomena.[2] For the shear-stress models of class (3), predictions have been confined to the isothermal, single-species plane flows, that is, to test cases 1, 4, 13, and 14.

The results of the calculations are shown in the figures of the appendix, which provide standard comparisons of predictions with experimental data for the four models of classes (1) and (2), and in figures 2 to 7 which display further aspects of particular predictions referred to in this discussion section. Also included in this section are a discussion of the relative success of the models in predicting the test flows, an examination of the models in ascending order of complexity (beginning with the Prandtl energy model) to discover in what respects a particular model is superior to the immediately preceding one, and a discussion of those features of the measurements which are not well predicted by any of the models and the possible reasons for the discrepancies.

The Prandtl Kinetic Energy Model (k)

Our experience of predicting wall boundary layers had led us to believe that there were scarcely any advantages in using Prandtl's kinetic energy model rather than his earlier mixing-length hypothesis; Mellor and Herring (ref. 12) reported a similar conclusion. Therefore, it should be emphasized that for free shear flows, the k model performs consistently better than the $m\ell h$ hypothesis. This fact is well brought out by reference to the jet predictions of cases 8, 12, and 18 and the wake-flow predictions of cases 13 to 16.

In concept, the k model represents a substantial advance over the $m\ell h$ hypothesis. That it is also superior in practice may be attributed to the fact that, in free shear flows but not in wall boundary layers, the convective transport and diffusive transport of kinetic energy are usually important terms in the energy-balance equation.

The foregoing remarks, however, are nearly the only ones that can be made in favor of the k model, inasmuch as reference to the cases noted indicates that there are still large discrepancies between the measured and calculated development of the flow. Invariably, over the initial region of a jet, the predicted rate of decay is too rapid; whereas, far downstream, the decay rate is too slow. The behavior over the initial region could, of course, be improved by choosing the length scale to be a smaller fraction of the flow width, but such a move would make the far-region predictions worse than ever.

---

[2] Jones and Launder (ref. 4) have in fact provided a low Reynolds number version of the $k\epsilon 1$ model; however, at several points in its derivation, the assumption is made that the low Reynolds number region is adjacent to a rigid surface as in wall boundary-layer flows. The model is thus not immediately applicable to free-shear-flow transition phenomena.

The Energy-Dissipation Model of Turbulence ($k\epsilon 1$)

The introduction of a transport equation for the dissipation rate removes the need to prescribe the length scale and leads to a model of turbulence possessing a much greater degree of universality than Prandtl's energy model, inasmuch as the length scale of turbulence is by no means a universal fraction of the width of the shear flow. Specifically, it is noted that, for many of the jet flows, the correct behavior is predicted both in the vicinity of the nozzle and many diameters downstream (cases 6, 9, 11, and 12). The $k\epsilon 1$ predictions of cases 13, 14, 15, 16, and 17 are also in distinctly better agreement with the data than are the k predictions.

The Extended Energy-Dissipation Model ($k\epsilon 2$)

When there is just one significant component of the velocity-gradient tensor and when the energy production and dissipation rates are approximately in balance, the $k\epsilon 1$ model nearly always gives acceptable predictions. The second condition is always met in wall boundary layers, in mixing layers, and also in many jet-like flows. When, however, the shear flow is weak (that is, when the excess or defect of the shear flow is but a small fraction of the velocity of the external stream), the model predicts too slow a decay rate of the shear flow; this behavior is exemplified in the predictions for cases 13, 15, 16, and 17 (the data for case 13 and for other similar but currently unpublished flows measured by Bradbury are shown replotted in fig. 2 in the format that the organizers adopted for the other weak shear flows).

Reference to the same test cases shows that much better agreement with data is achieved with the $k\epsilon 2$ model. Distinct improvements may also be seen in the predictions of cases 11, 12, and 19. The result is particularly encouraging in that Rodi (ref. 8) determined the C_μ function without reference to the data considered at this conference.

The Stress Models of Turbulence ($\overline{u_i u_j}\epsilon$ and $\overline{uv}k\epsilon$)

Models of this class have been applied to only four of the flows so that inferences drawn must be more tentative than those for the models already discussed. Moreover, when this set of computations was made, little time remained before the conference deadline and, consequently, only a preliminary adjustment of the constants was possible.

Predictions for all models gave results for case 1 scarcely distinguishable from those obtained with the $k\epsilon$ viscosity models. For case 4 (standard comparisons shown in fig. 3), however, the stress models do give a small but definite improvement; the fact emerges clearly in figure 4 which shows the development of the minimum velocity with

distance downstream. The stress models[3] follow the measured development very closely, whereas the $k\epsilon 2$ predictions show initially too steep a rise and, later, a too gradual disappearance of the wake.

The other two sets of predictions are for flows which, superficially at any rate, are very similar; yet they would lead one to draw different conclusions about the relative correctness of the models. It is seen from figures 5 and 6 that the models which are best at predicting case 13 are worst for case 14 and vice versa.[4] The experimental data from both sets of investigations seem admirably consistent. Perhaps, therefore, the differences in the development of the two flows may be traced to the different initial shear flows from which they develop, namely, a mixing layer for case 13 and a wall boundary layer for case 14. Certainly it is known from parallel research at Imperial College that none of the pressure-strain approximations so far employed predict the normal-stress profiles well close to a wall; thus, possibly there is some residual influence of the wall in the initial region of case 14.

The profiles of the lateral and streamwise energy components for case 14 are compared with the experimental data in figure 7. Agreement with the data may be thought reasonably good. It is not believed possible, on the basis of the calculations made so far, to determine which of the approximations for the diffusion and pressure-strain correlations is the best. The proposal of Naot and coworkers (ref. 13) and Reynolds (ref. 14) for the pressure-strain correlation is simple and, for the four test cases examined, not discernibly worse than the other two. It seems likely, however, that a more elaborate form, akin to stress-model versions B and C, will be needed if the axisymmetric and plane flows are to be well predicted with a single set of constants.

Aspects of the Flows Which are Poorly Predicted

The most serious disagreements between the $k\epsilon 2$ predictions and measurements arise in flows where there are appreciable density gradients. Cases 5 and 7 both suggest that compressibility effects reduce, somewhat, the rate of spread of a mixing layer, whereas the $k\epsilon 2$ model indicates no significant variation with Mach number. This trend is not uniform over all the flows. However, the predictions of the jets of cases 19 and 12 both display reasonable agreement with the experimental data; whereas, the experiments of cases 10 and 21 exhibit a jet decay much faster than the predictions herein would indicate.

---

[3] The letter and number ascribed to the $\overline{u_i u_j}\epsilon$ models denote the versions of the diffusion and pressure-strain hypotheses which were employed. (See table 6.)

[4] The only reason that the $k\epsilon 2$ model gave good predictions for both flows was that the initial value of $g\left(\overline{P/\epsilon}\right)$ was raised to 1.2 for case 14.

At least some of these contradictions may be attributed to the difficulty of prescribing adequately the initial conditions, particularly for the hydrogen jets of cases 10 and 21 where calculations start nearly 3 diameters downstream from the exit. An additional prediction of these flows has been made, in which the initial values of k and μ_t across the jet have been doubled. The resultant predictions shown on the standard comparison are in much closer agreement with experimental data than those previously obtained with the $k\epsilon 2$ model. Moreover, if the turbulent Prandtl/Schmidt number had been taken as 0.5 rather than 0.7 (the former value was adopted with the k and $ml h$ models), the prediction of the velocity decay would have been further improved.

Apparently, little success has been had with any of Chriss and Paulk's data inasmuch as their air/air jet (case 20) also decays much faster than the $k\epsilon 2$ predictions herein show. Since computations are begun right at the jet lip, initial conditions have little effect on the flow for case 20. The rate of spread is, however, quite sensitive to the presence of turbulence in the core region. Included in the standard comparison for this flow is a prediction where the initial turbulence intensity $\left(\sqrt{\overline{u^2}}/U_o\right)$ was about 5 percent. It may be seen that this curve follows more closely the experimental data over the first 8 diameters or so.

Predictions are also in poor agreement with experimental data for the hydrogen jet of case 22. The flow is interesting because, through the presence of boundary layers on the nozzle walls, the "jet" actually has a momentum deficit. This discrepancy may be attributable to (1) the initial value of μ_t being too high (the effect of halving it is shown) and (2) the initial velocity profile having too small a momentum deficit.

For the uniform-density flows, disagreement between experiment and prediction is much less. The following discrepancies however are to be noted:

Case 4: The predicted shear stress at the downstream station is only half the measured. In view of the excellent predictions of the velocity profiles achieved by the stress models, it is difficult to accept that the predicted shear-stress profile can be much in error.

Case 14: It seems that the momentum deficit of the wake measured at $x = 1.5$ m may be rather more than that at the other stations.

Case 15: The near-wake behavior is not well predicted for this case, probably because of the pressure gradient across the boundary layer. In the calculations herein, zero cross-stream pressure variation is presumed.

Case 18: The predictions of the turbulence energy show a flatter top to the profile than do the standard data. It is seen that Rodi's (ref. 15) recent measurements, employing what is claimed to be a more accurate signal-processing technique, are in closer agreement with the prediction.

Case 23: For this case, the experimental data show a progressive loss of momentum as the flow develops downstream.

CONCLUSIONS

The following main conclusions can be drawn from this work:

1. Turbulence models which determine the length scale of turbulence from the transport equation for energy dissipation rate (or from some other length-scale-containing variable) can give correct predictions over a wider range of flows than is possible with models embodying algebraic prescriptions of l.

2. The $k\epsilon 2$ model, which incorporates the dependence of C_μ on $\left(\overline{P/\epsilon}\right)$, leads to reasonable predictions of both strong and weak free shear flows.

3. The versions of the Reynolds stress models which were tested already give, on the average, predictions for the four cases considered which are slightly superior to those of the $k\epsilon 1$ model. There is, however, evident need for further refinement, particularly with respect to the pressure-strain approximation.

4. More experiments are needed on flows with density variation in order to resolve the question of whether or not there is a systematic influence of density variation for which the present models do not account.

5. It is very desirable that experimenters should measure and report the distributions of turbulence quantities at the upstream boundaries of the flows, as well as just the time-mean velocities, temperatures, and compositions.

ACKNOWLEDGMENTS

The support of the Science Research Council is gratefully acknowledged through Research Grant B/RG/1863 and through the award of an SRC Research Studentship to A. Morse.

The computations were performed by means of digital computers under the control of the University of London Computer Centre.

Valuable assistance in the computations was provided by Mr. J. N. Loughhead; to him the authors offer their sincere thanks.

APPENDIX

PREDICTIONS OF TEST CASES 1 TO 23

This appendix contains, in order, predictions of test cases 1 to 23, obtained with the aid of the four turbulent-viscosity models. (See pages 697 and 698 for index to test cases.)

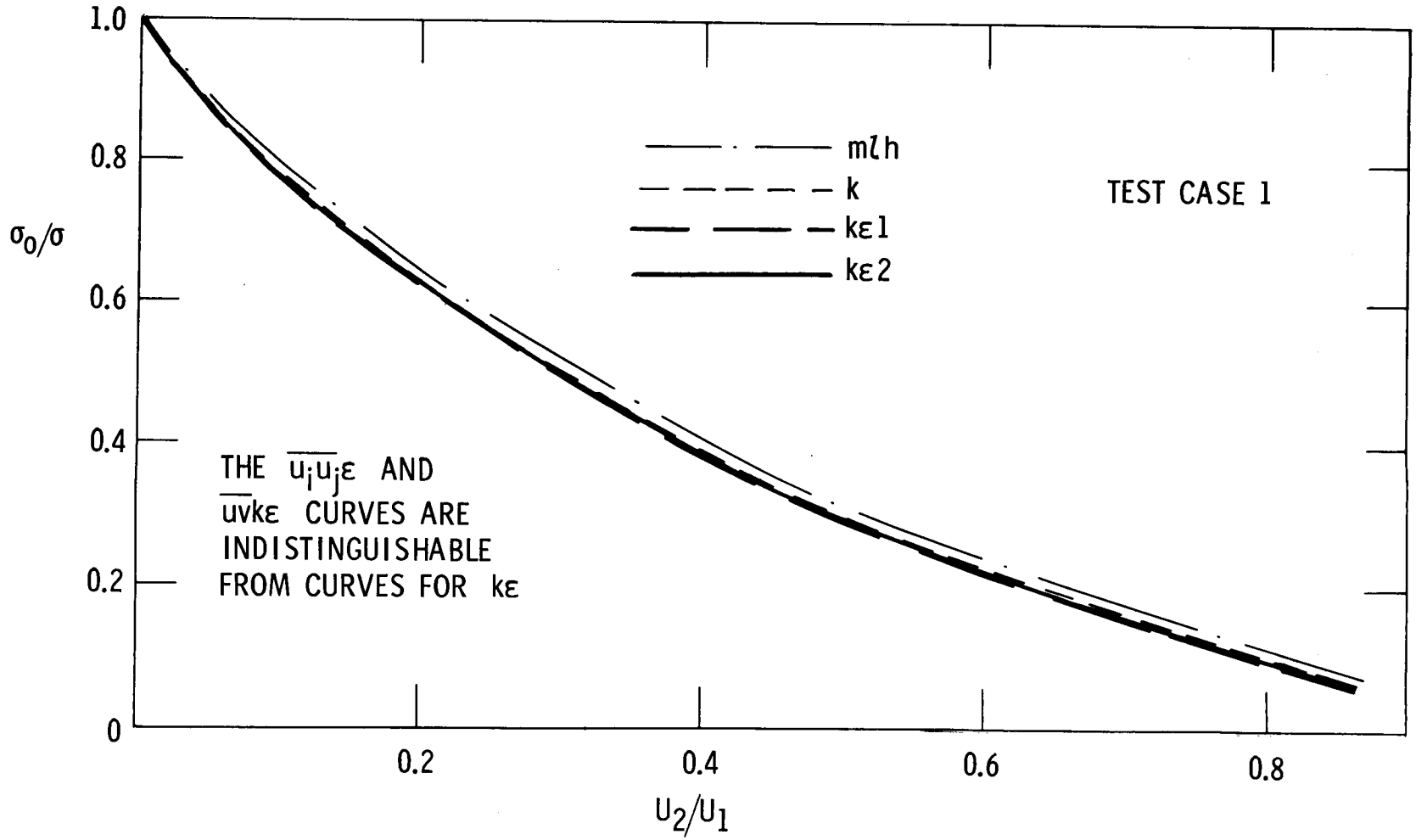
1.0
0.8
0.6
0.4
0.2
0
σ_0/σ
0.2
0.4
0.6
0.8
U_2/U_1
mlh
k
kε1
kε2
TEST CASE 1
THE $\overline{u_i u_j}\varepsilon$ AND
$\overline{uv}k\varepsilon$ CURVES ARE
INDISTINGUISHABLE
FROM CURVES FOR kε

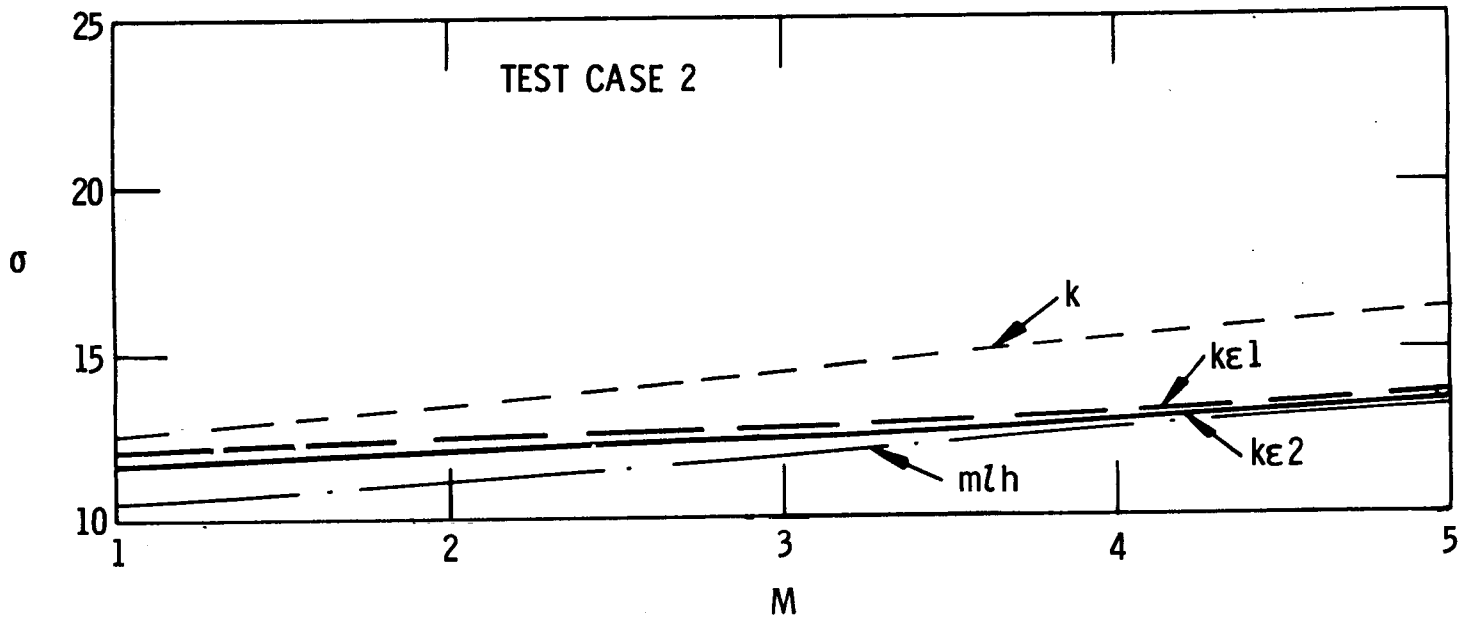
TEST CASE 2
25
20
15
10
σ
1
2
3
4
5
M
k
kε1
kε2
mℓh

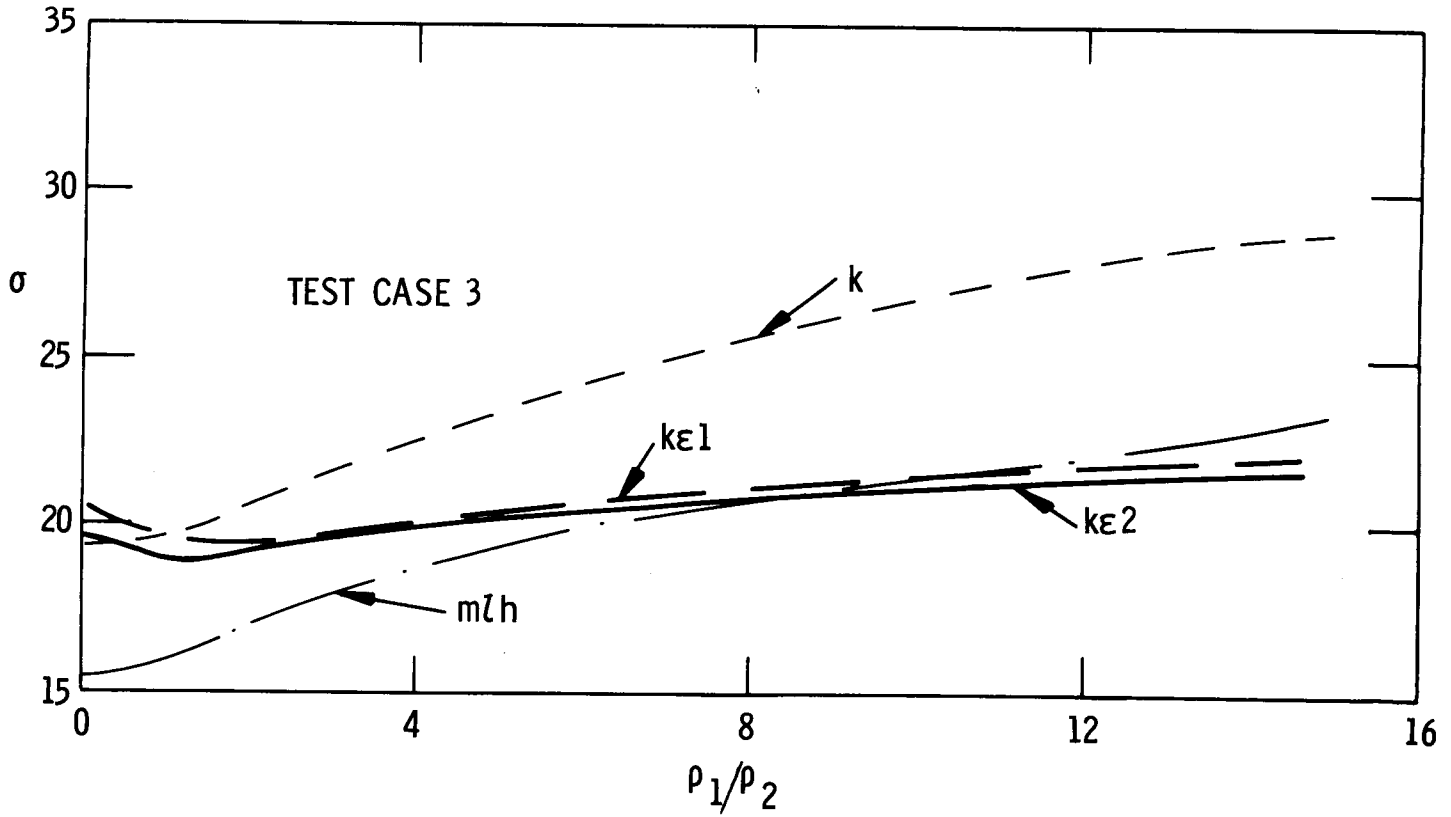
35
30
25
20
15
σ
TEST CASE 3
k
kε1
kε2
mℓh
0
4
8
12
16
ρ1/ρ2

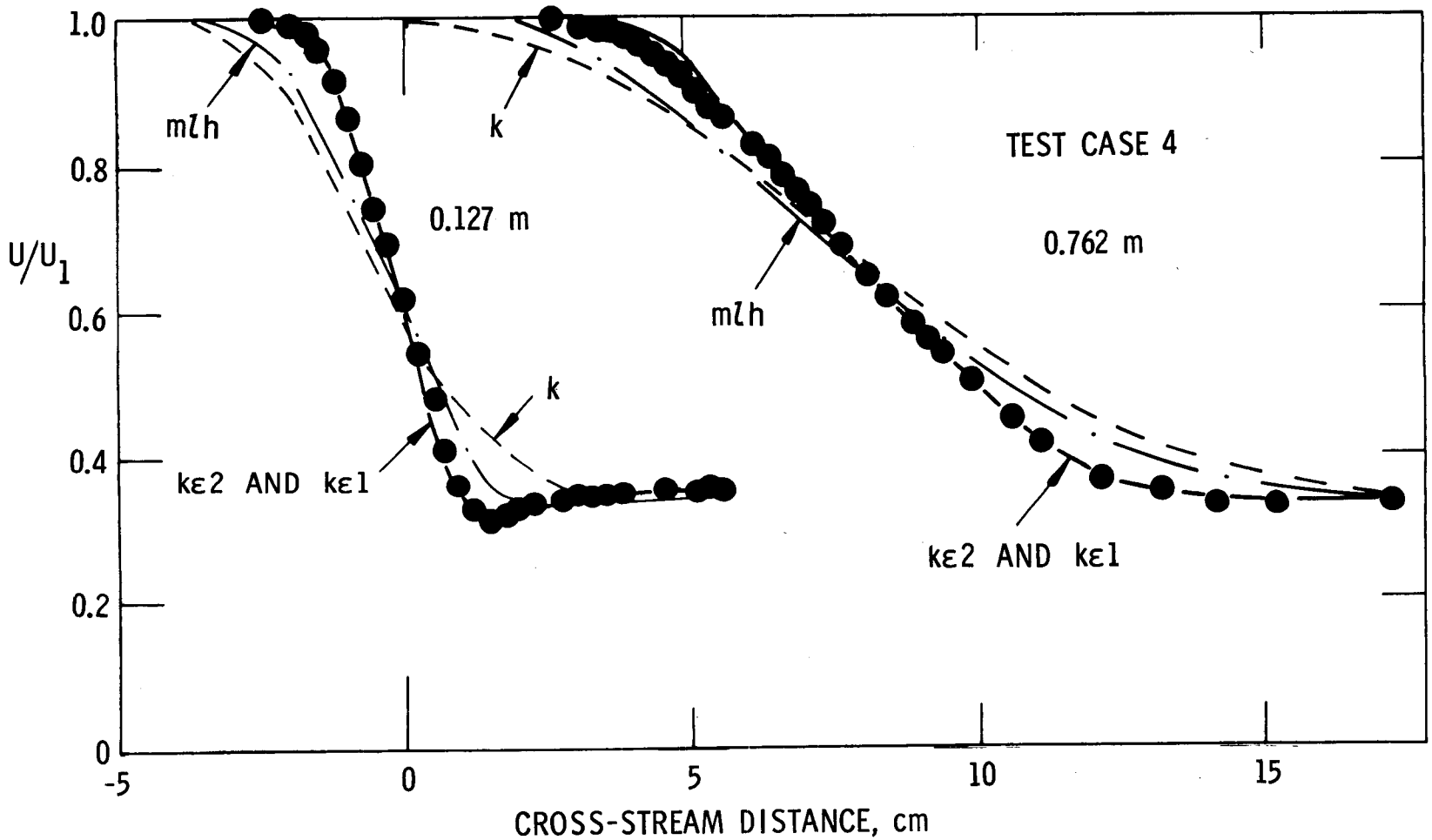
1.0
0.8
0.6
0.4
0.2
0
U/U1
mlh
k
0.127 m
kε2 AND kε1
k
TEST CASE 4
0.762 m
mlh
kε2 AND kε1
-5
0
5
10
15
CROSS-STREAM DISTANCE, cm

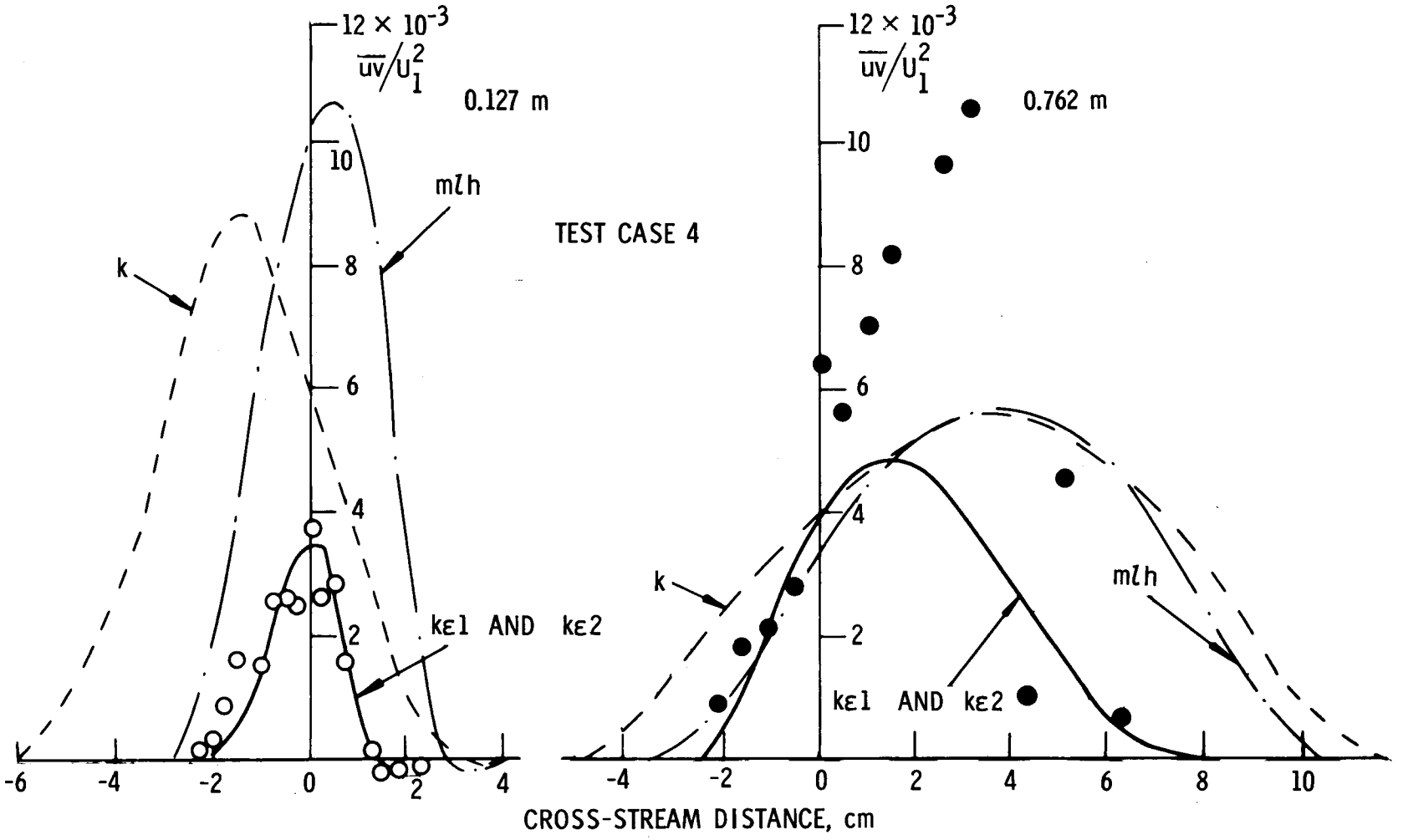
12×10^{-3}
$\overline{uv}/U_1^2$
0.127 m
10
8
6
4
2
mℓh
k
kε1 AND kε2
-6
-4
-2
0
2
4
TEST CASE 4
12×10^{-3}
$\overline{uv}/U_1^2$
0.762 m
10
8
6
4
2
k
mℓh
kε1 AND kε2
-4
-2
0
2
4
6
8
10
CROSS-STREAM DISTANCE, cm

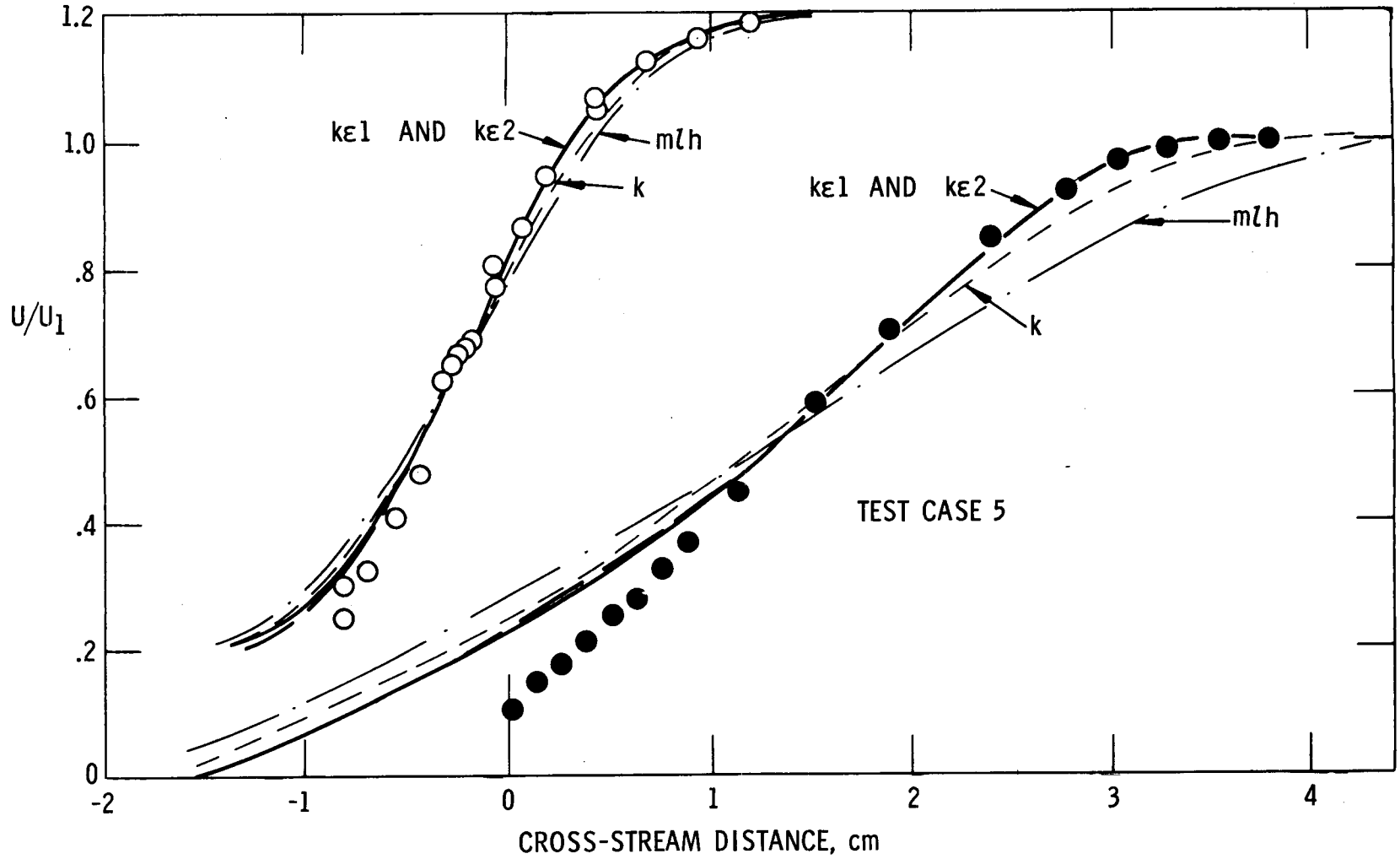
1.2
1.0
.8
.6
.4
.2
0
U/U1
kε1 AND kε2
mlh
k
kε1 AND kε2
mlh
k
TEST CASE 5
-2
-1
0
1
2
3
4
CROSS-STREAM DISTANCE, cm

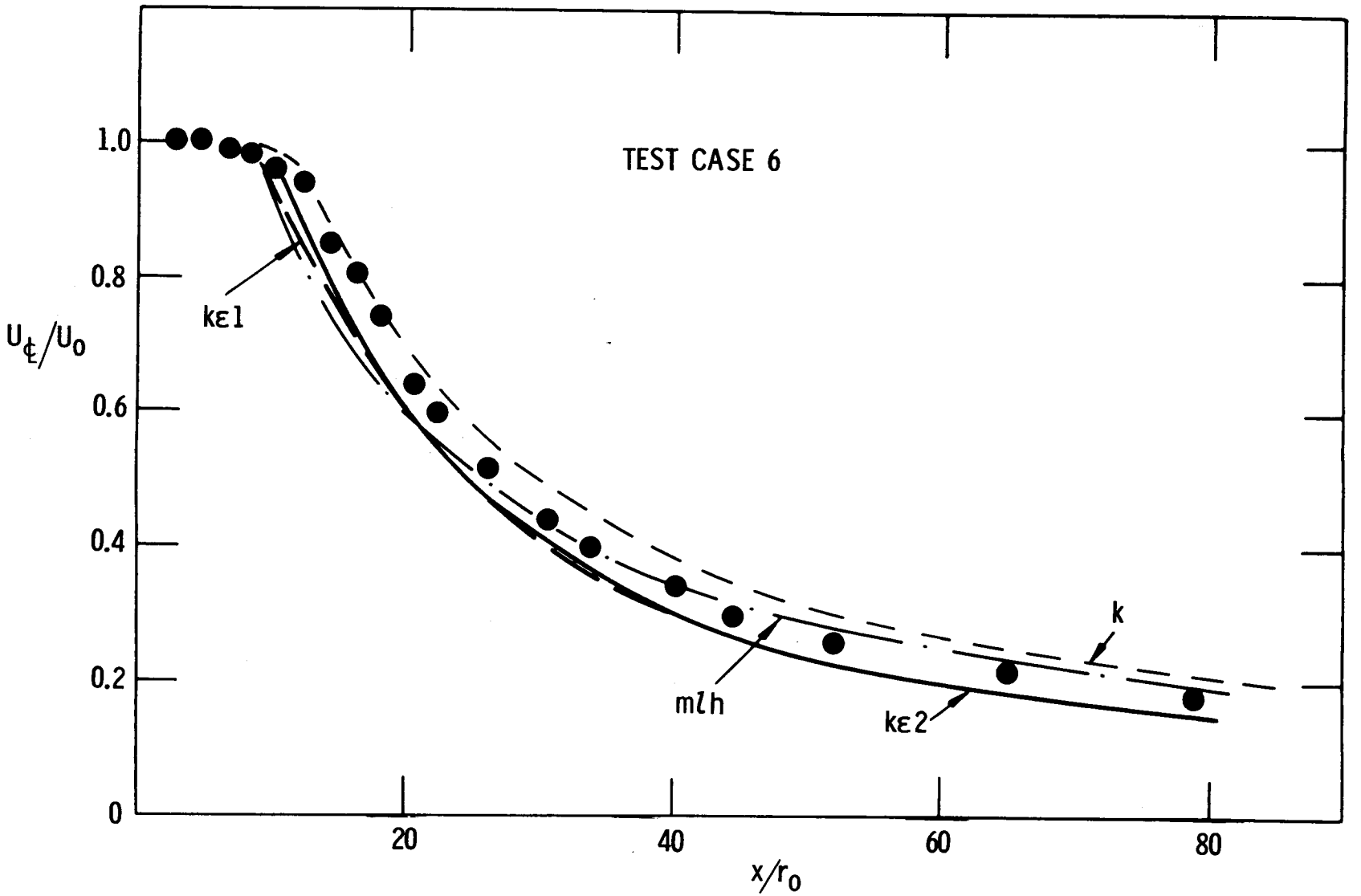
TEST CASE 6
1.0
0.8
0.6
0.4
0.2
0
U_{ℓ}/U_0
kε1
k
mℓh
kε2
20
40
60
80
x/r_0

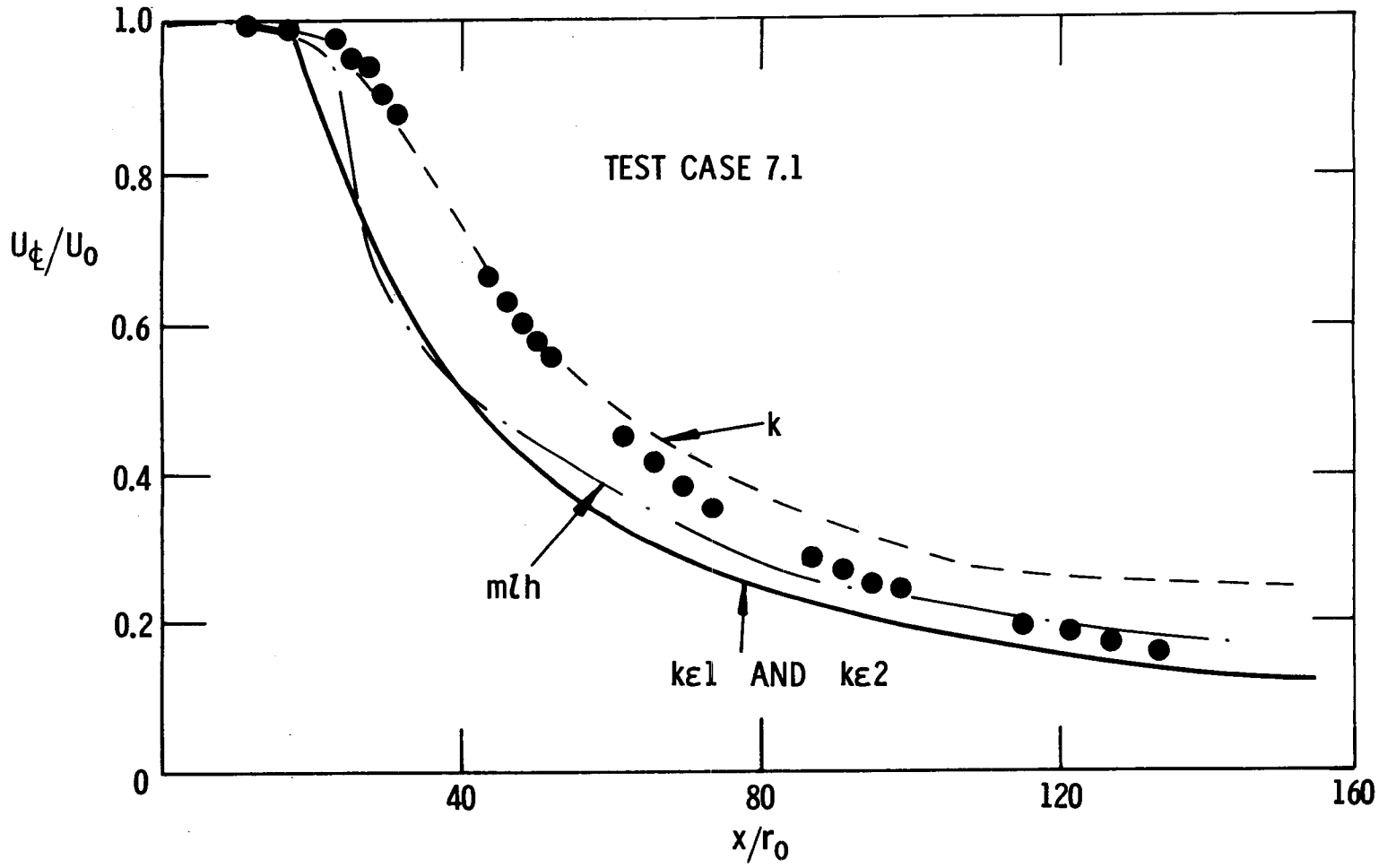
TEST CASE 7.1
U_{ℓ}/U_0
1.0
0.8
0.6
0.4
0.2
0
40
80
120
160
x/r_0
k
mlh
kε1 AND kε2

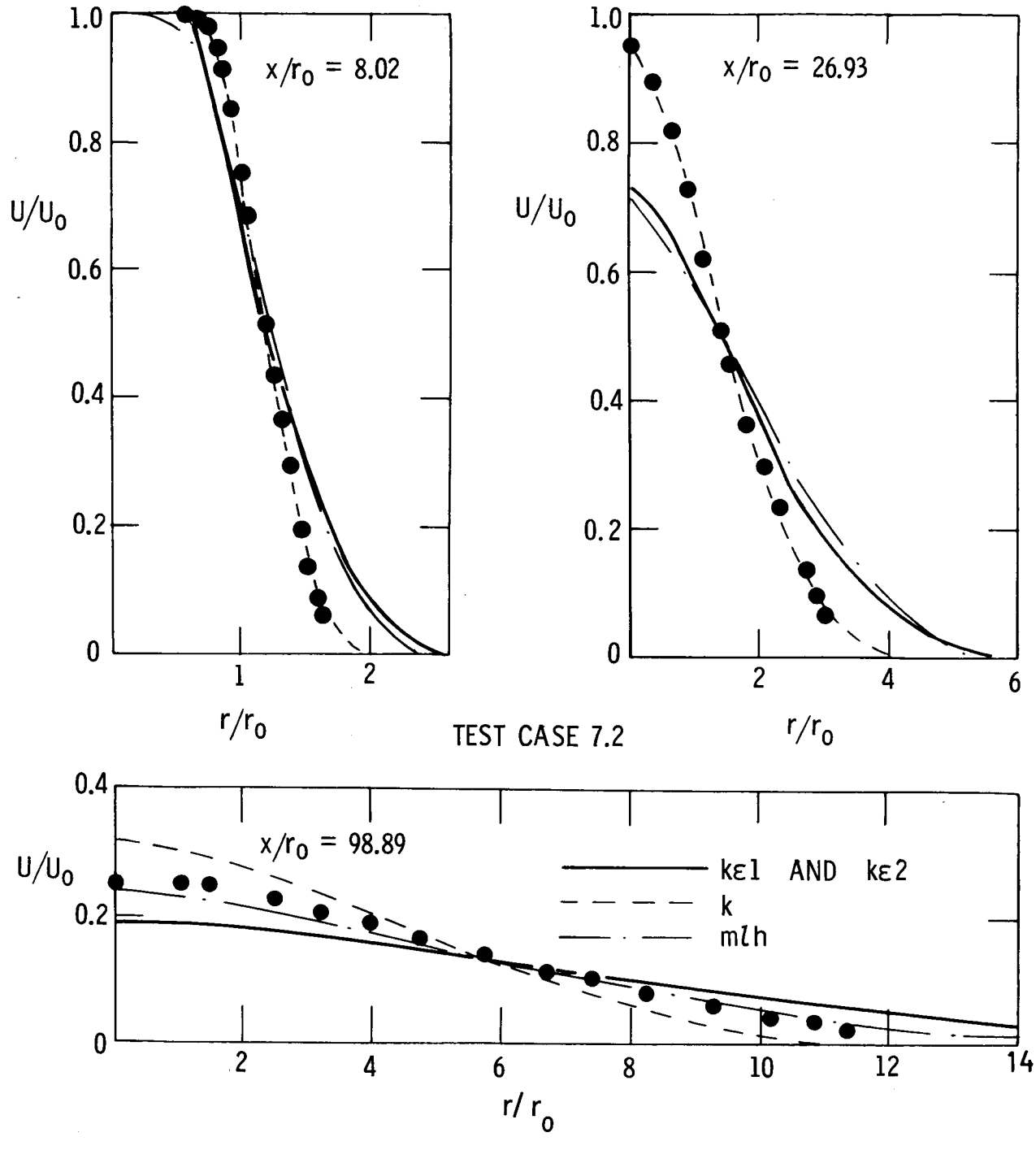
1.0
0.8
0.6
0.4
0.2
0
U/U0
x/r0 = 8.02
1
2
r/r0
x/r0 = 26.93
2
4
6
TEST CASE 7.2
0.4
x/r0 = 98.89
kε1 AND kε2
k
mlh
2
4
6
8
10
12
14
r/ r0

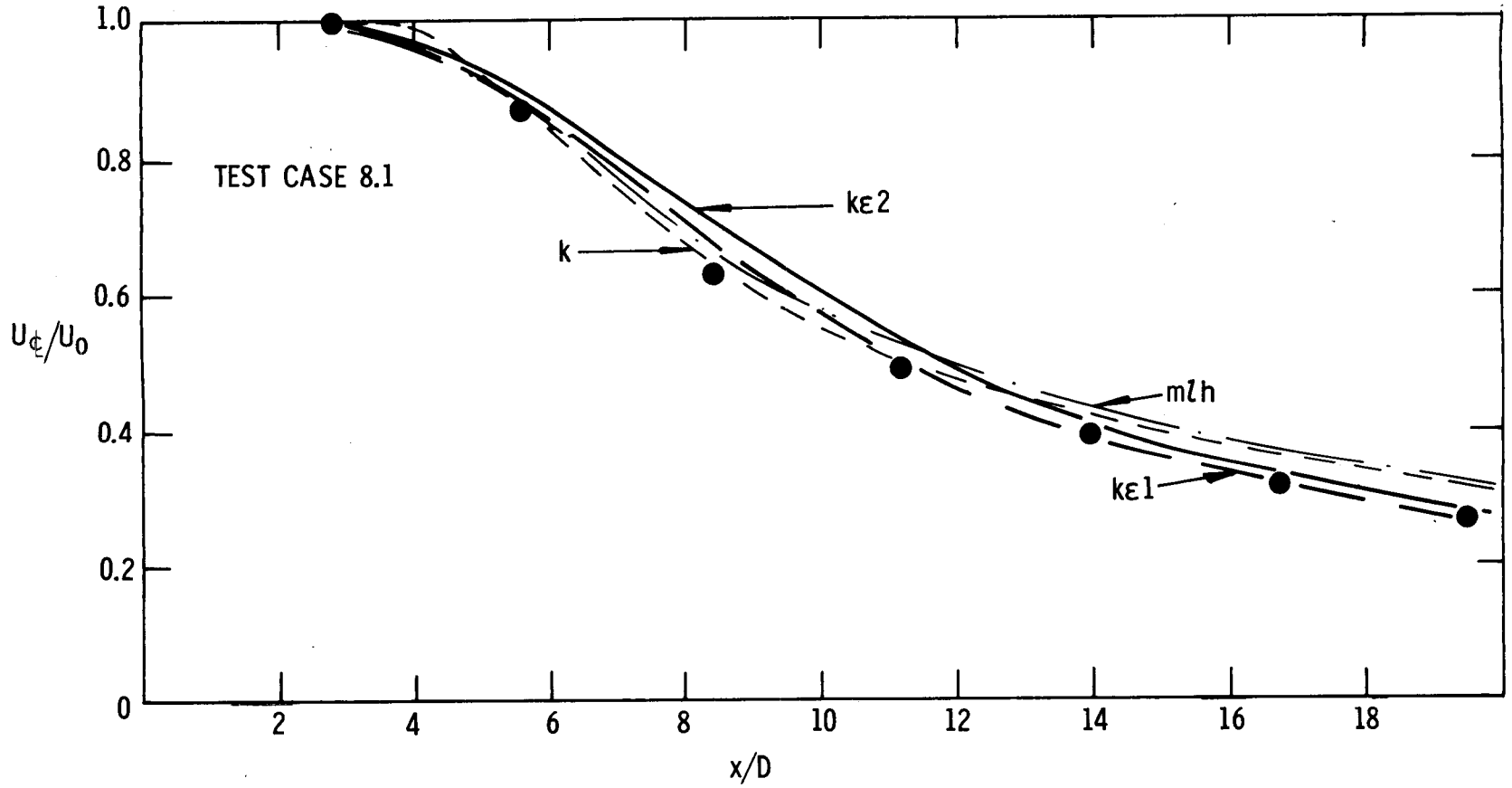
TEST CASE 8.1
kε2
k
mlh
kε1
U_{ℓ}/U_0
x/D
1.0
0.8
0.6
0.4
0.2
0
2
4
6
8
10
12
14
16
18

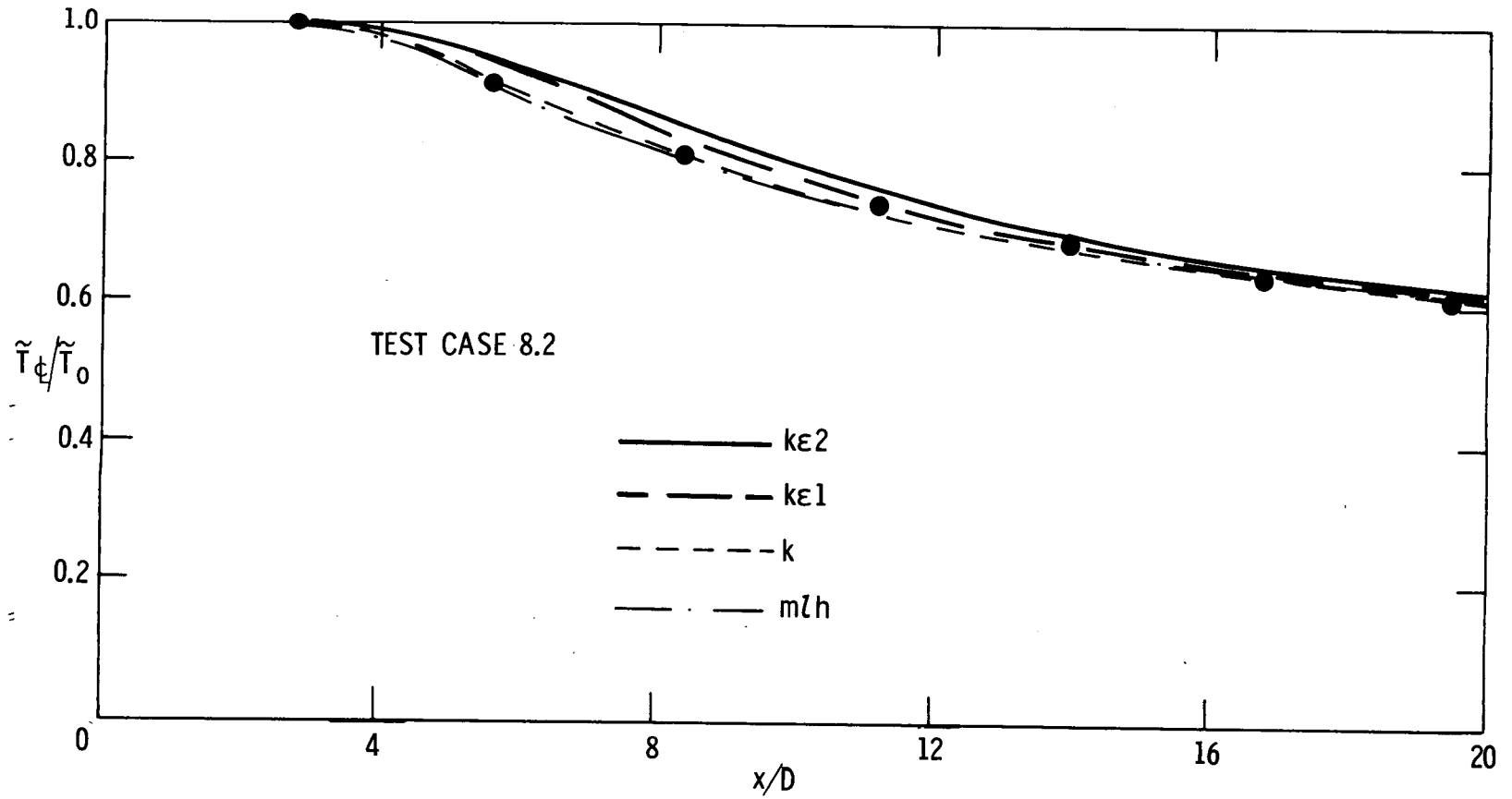
1.0
0.8
0.6
0.4
0.2
0
$\tilde{T}_{\ell}/\tilde{T}_0$
TEST CASE 8.2
kε2
kε1
k
mlh
4
8
12
16
20
x/D

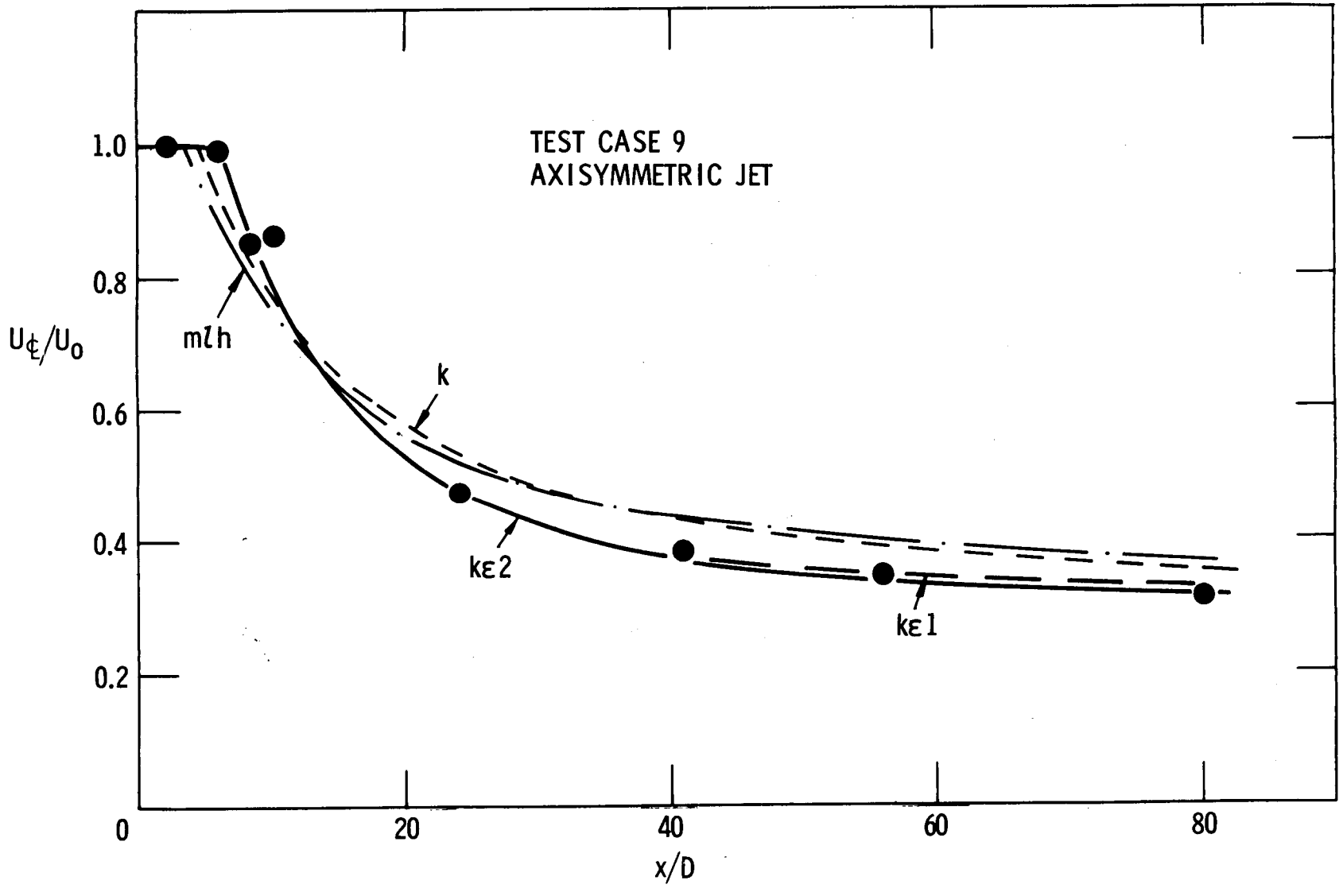
TEST CASE 9
AXISYMMETRIC JET
1.0
0.8
0.6
0.4
0.2
0
U_{ℓ}/U_0
mℓh
k
kε2
kε1
20
40
60
80
x/D

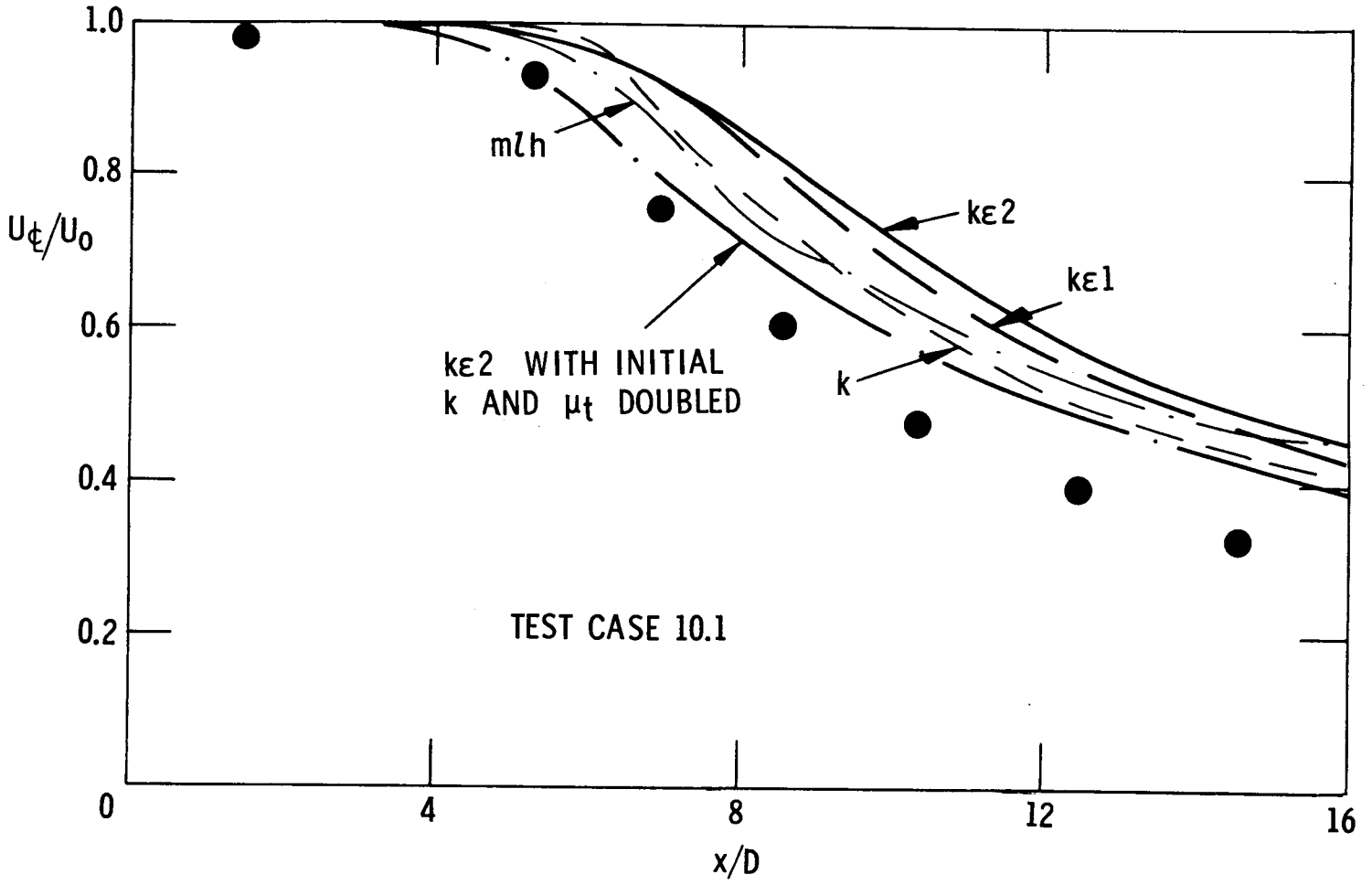
1.0
0.8
0.6
0.4
0.2
0
U_{ℓ}/U_0
4
8
12
16
x/D
mlh
kε2
kε1
k
kε2 WITH INITIAL
k AND μ_t DOUBLED
TEST CASE 10.1

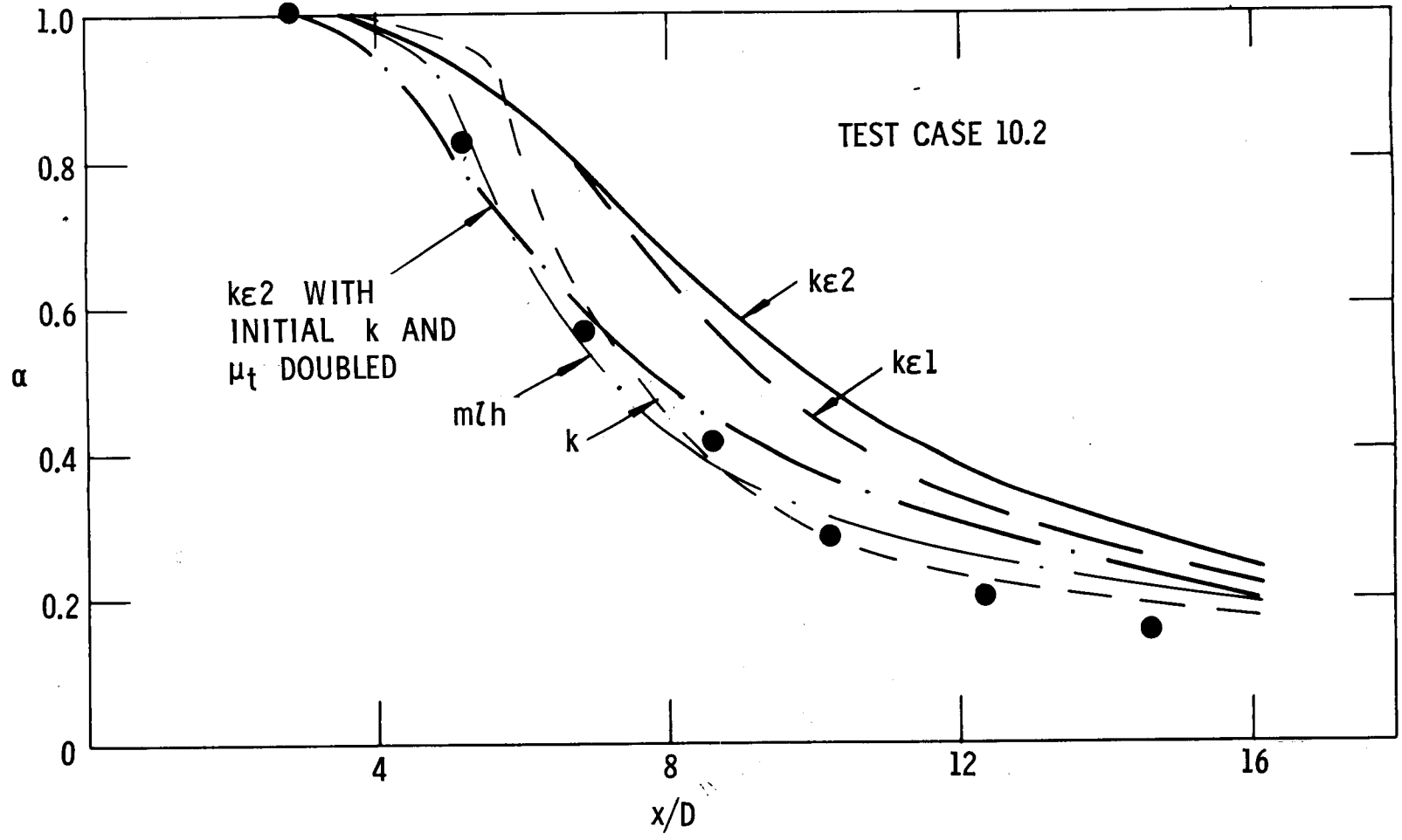
TEST CASE 10.2
kε2 WITH
INITIAL k AND
μ_t DOUBLED
kε2
kε1
mlh
k
α
x/D
1.0
0.8
0.6
0.4
0.2
0
4
8
12
16

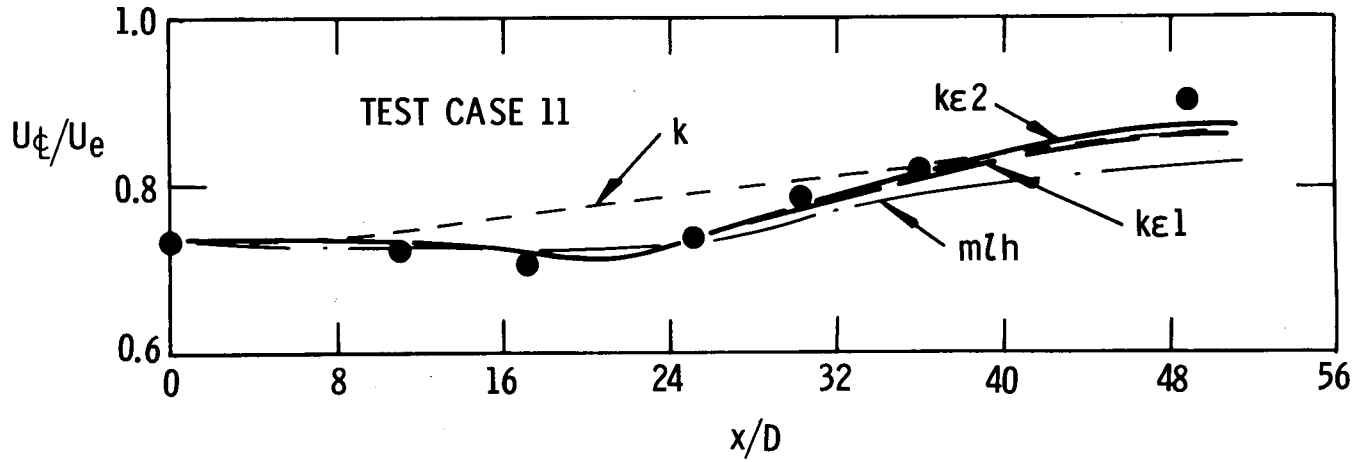
1.0
0.8
0.6
U_{ℓ}/U_e
TEST CASE 11
k
kε2
kε1
mlh
0
8
16
24
32
40
48
56
x/D

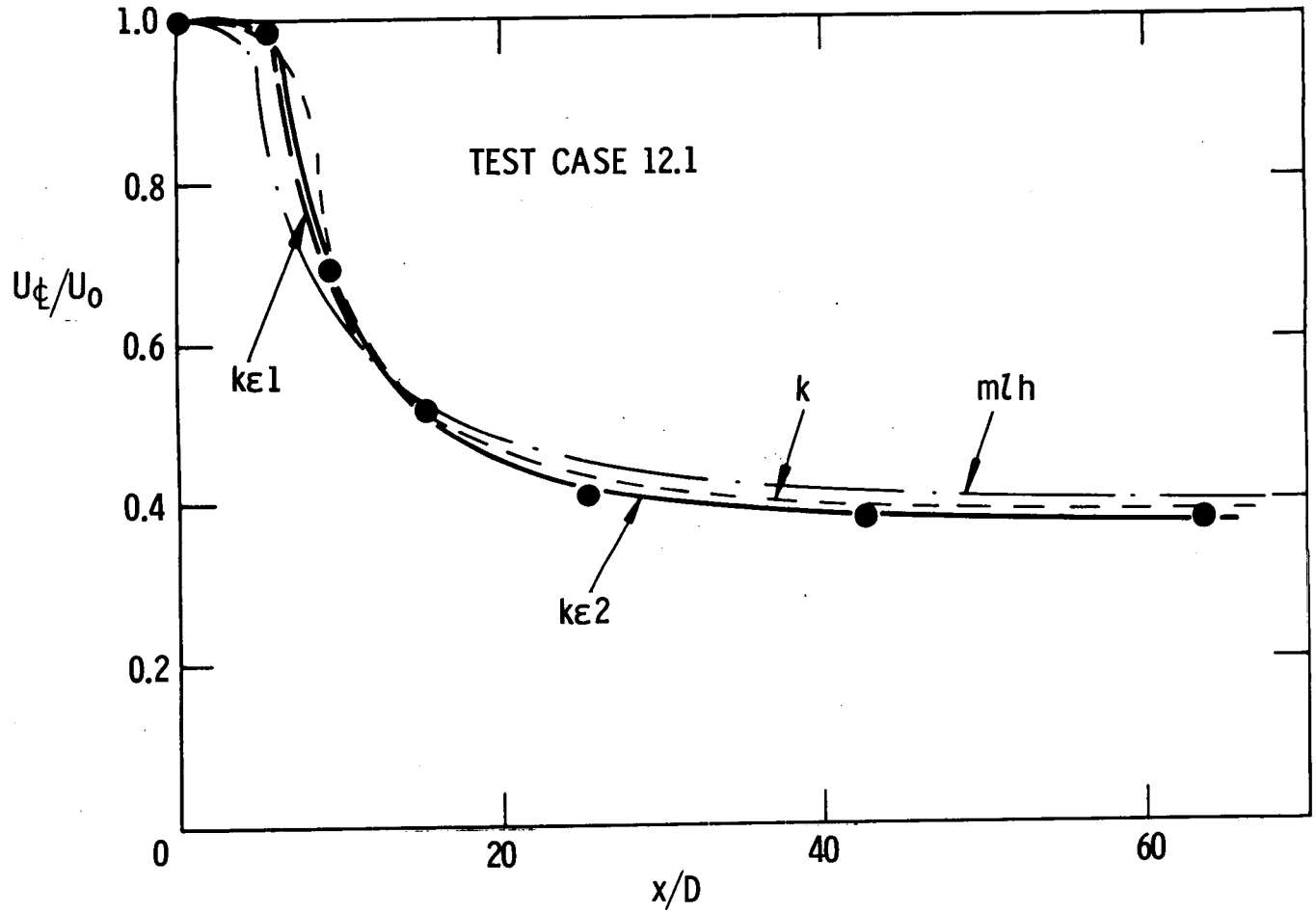
TEST CASE 12.1
U_{ℓ}/U_0
1.0
0.8
0.6
0.4
0.2
0
20
40
60
x/D
kε1
k
mℓh
kε2

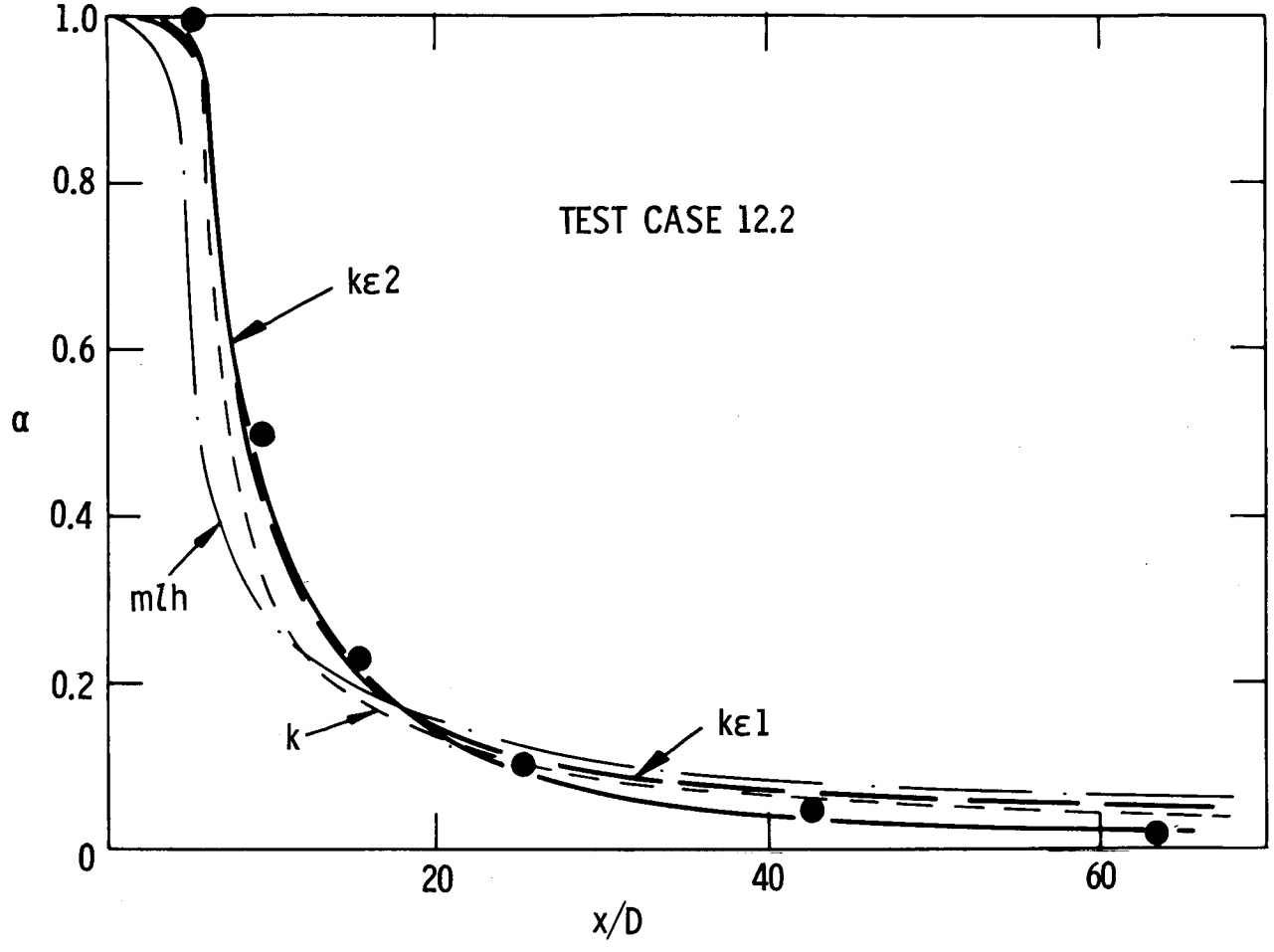
TEST CASE 12.2
kε2
mℓh
k
kε1
α
x/D
1.0
0.8
0.6
0.4
0.2
0
20
40
60

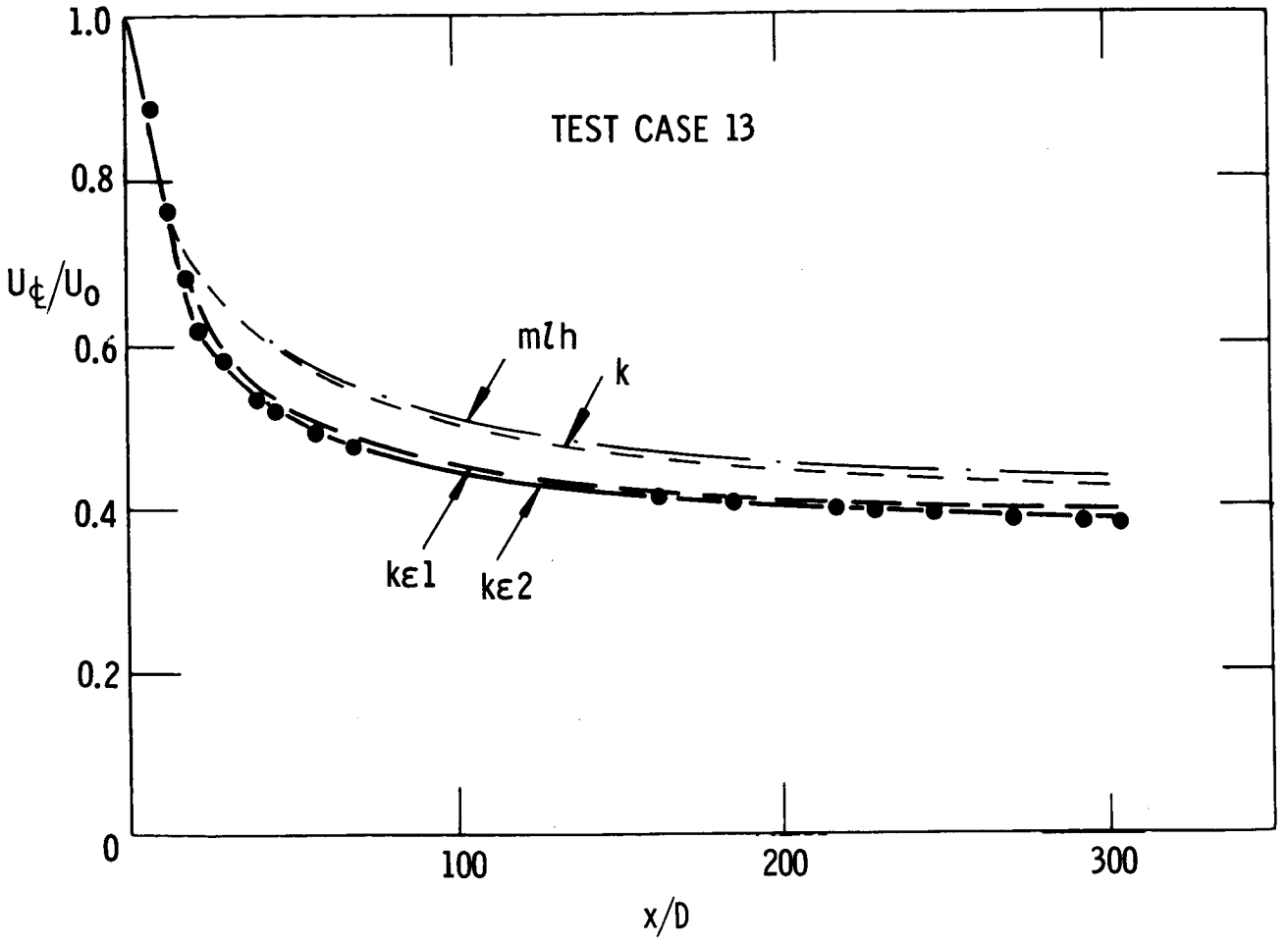
TEST CASE 13
1.0
0.8
0.6
0.4
0.2
0
U_{ℓ}/U_o
mlh
k
kε1
kε2
100
200
300
x/D

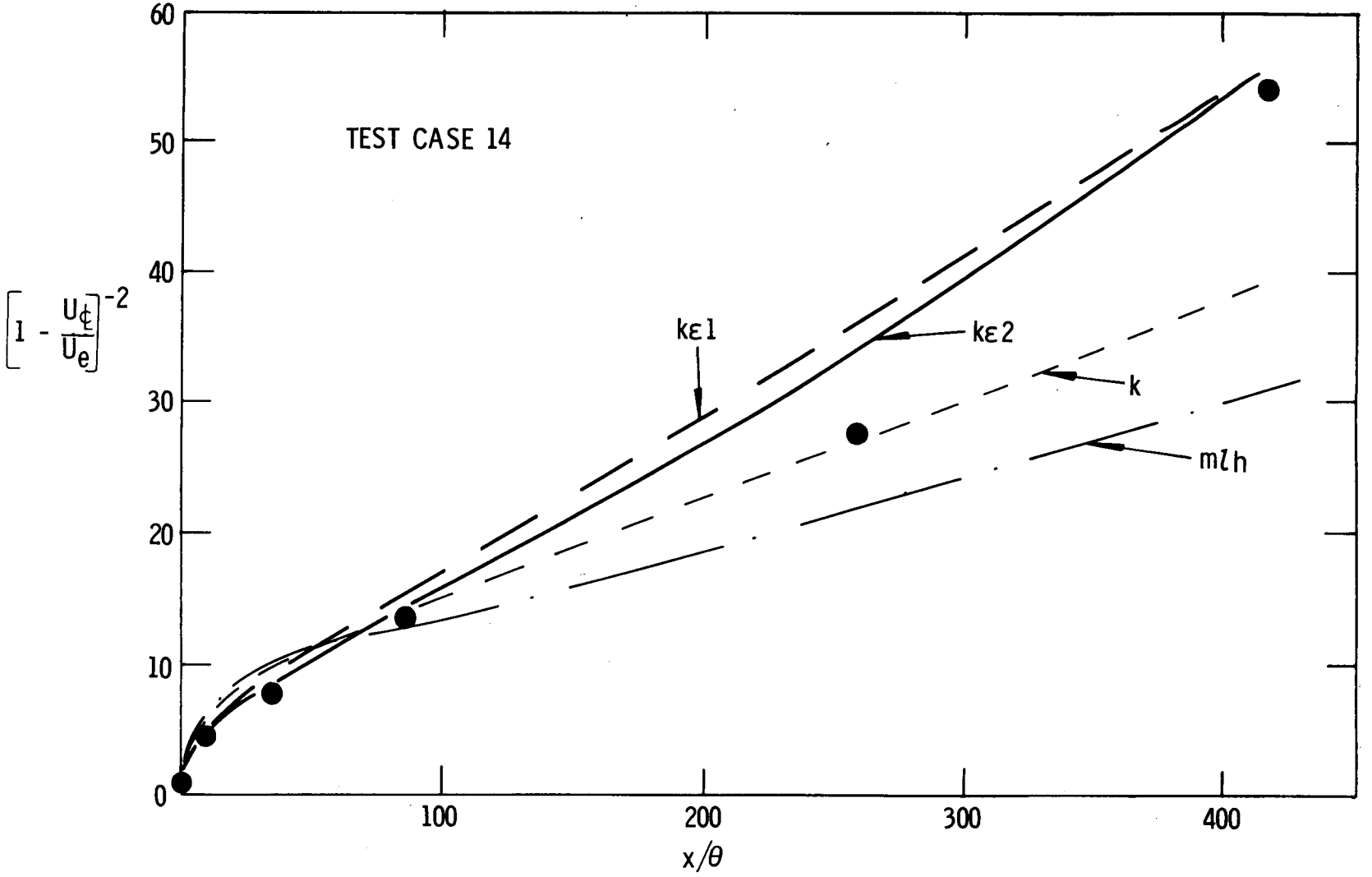
TEST CASE 14
$\left[1 - \frac{U_\ell}{U_e}\right]^{-2}$
60
50
40
30
20
10
0
100
200
300
400
x/θ
kε1
kε2
k
mlh

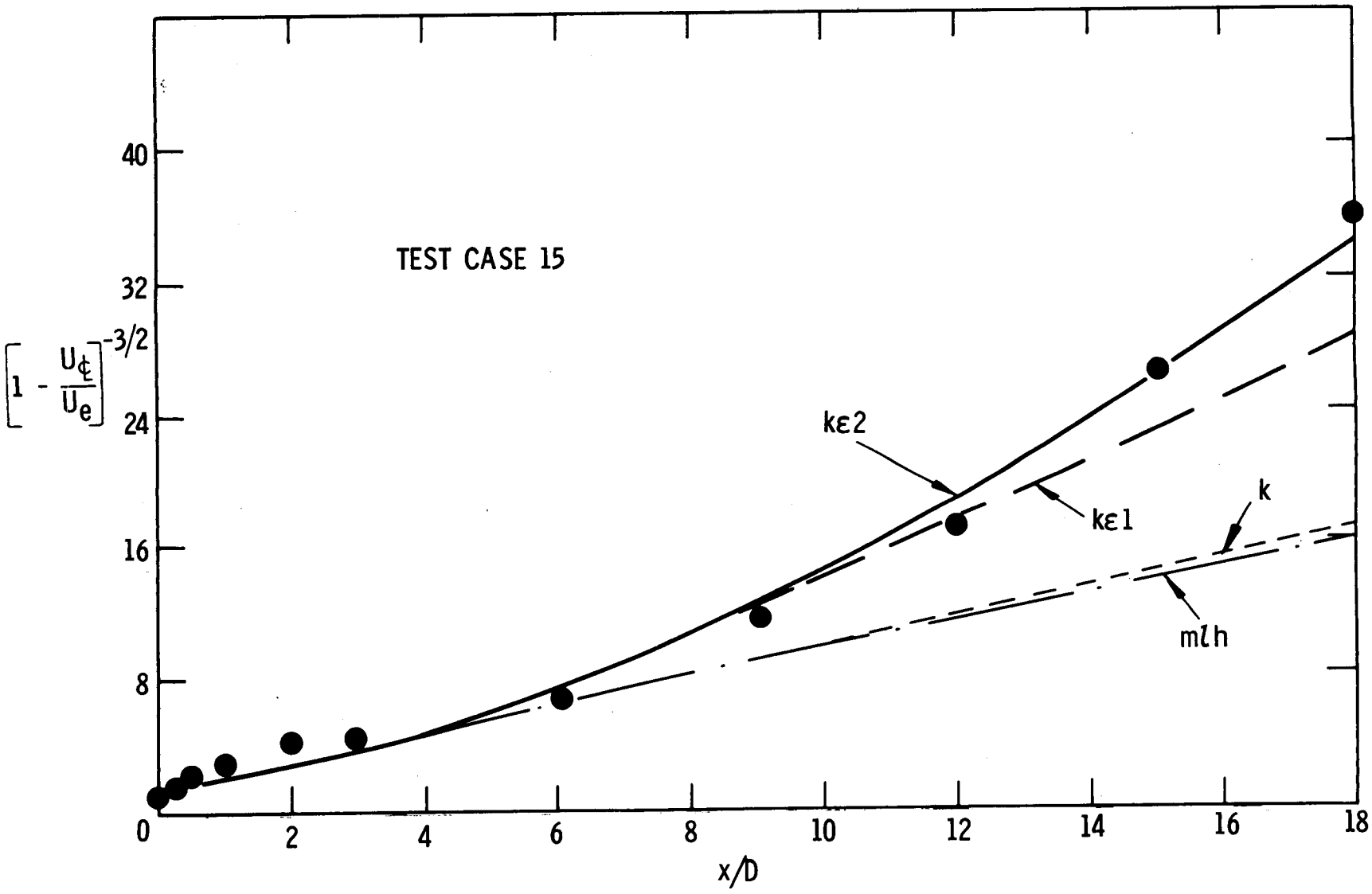
TEST CASE 15
$\left[1 - \frac{U_\ell}{U_e}\right]^{-3/2}$
40
32
24
16
8
0
2
4
6
8
10
12
14
16
18
x/D
kε2
kε1
k
mlh

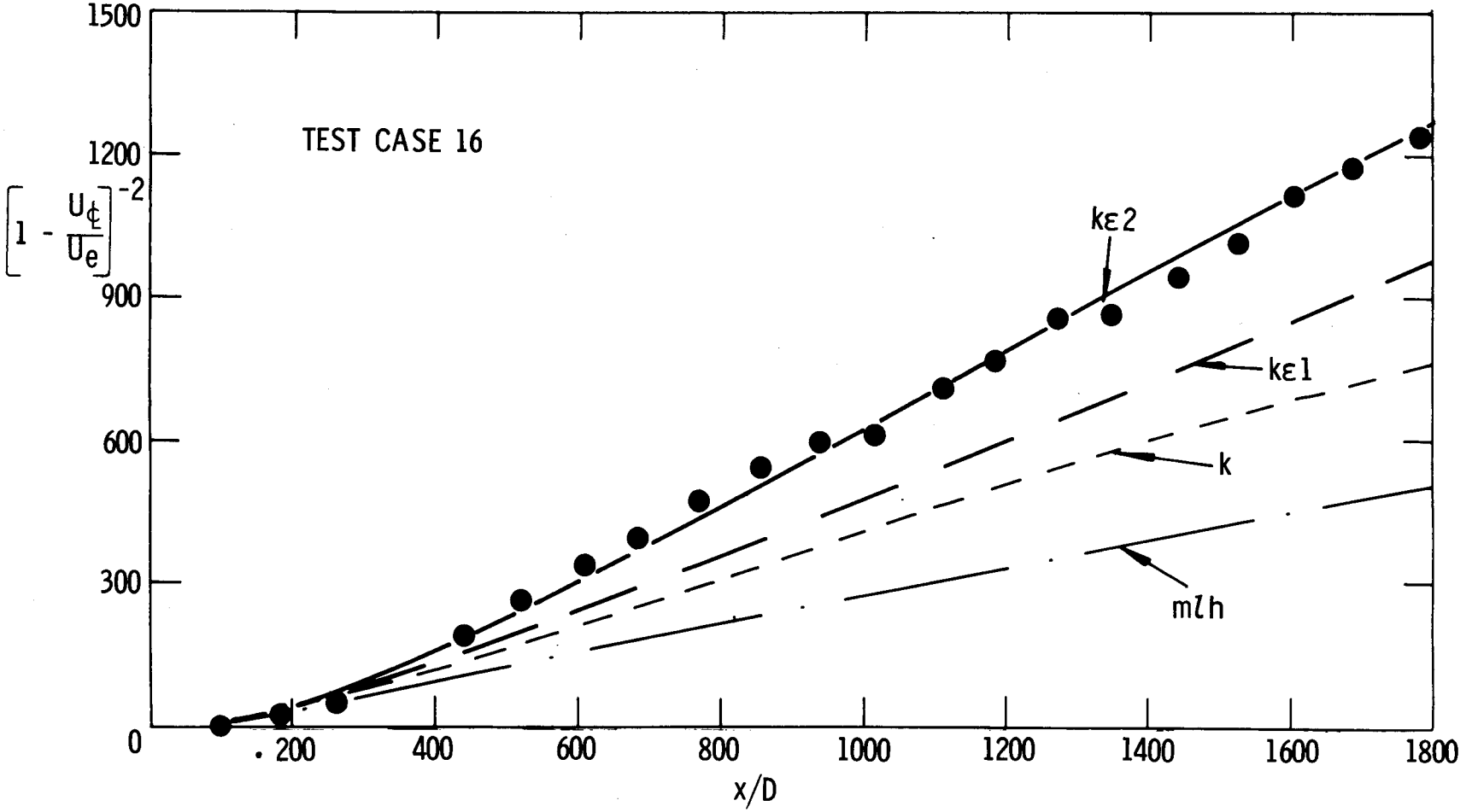
TEST CASE 16
$\left[1 - \frac{U_\phi}{U_e}\right]^{-2}$
1500
1200
900
600
300
0
200
400
600
800
1000
1200
1400
1600
1800
x/D
kε2
kε1
k
mlh

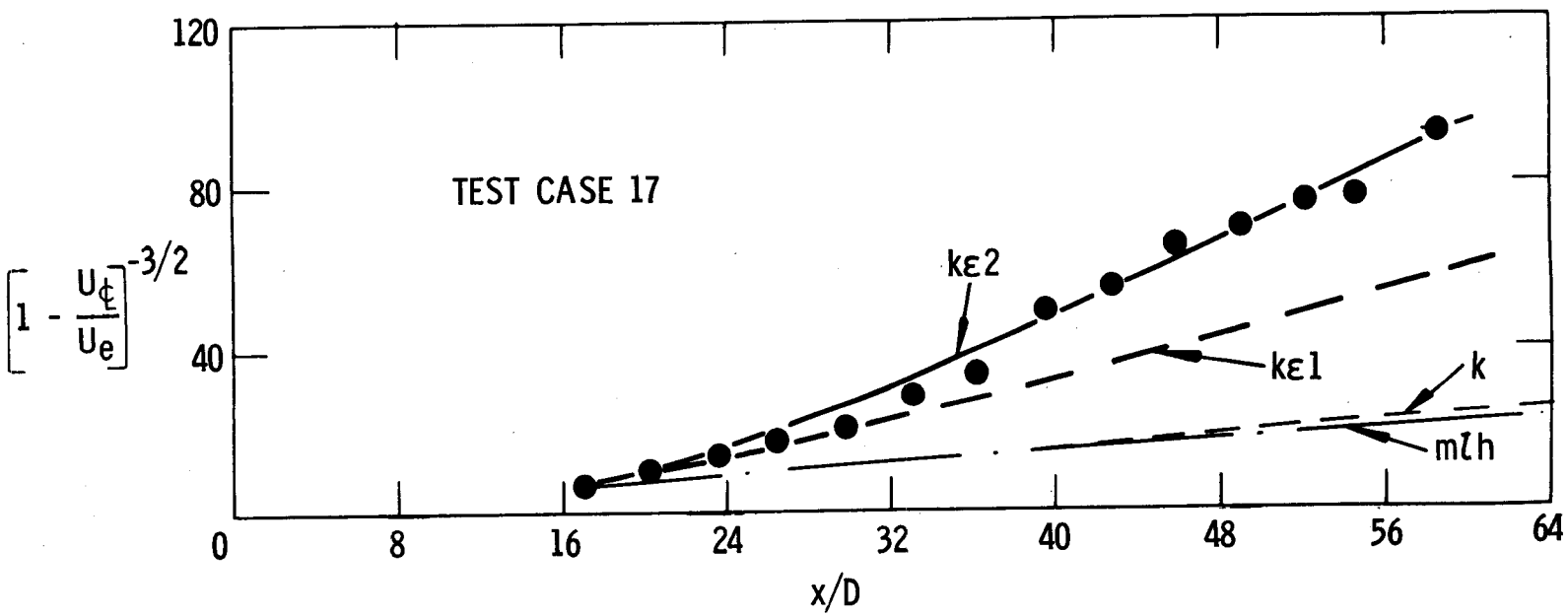
TEST CASE 17
$\left[1 - \frac{U_{\ell}}{U_e}\right]^{-3/2}$
120
80
40
0
8
16
24
32
40
48
56
64
x/D
kε2
kε1
k
mℓh

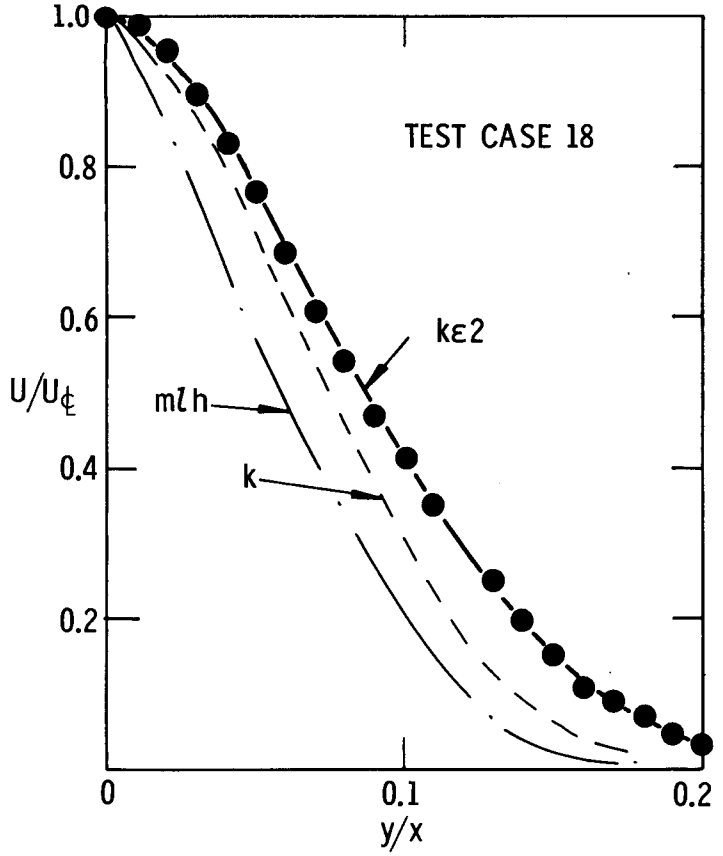
1.0
0.8
0.6
0.4
0.2
U/U℄
TEST CASE 18
kε2
mlh
k
0
0.1
0.2
y/x

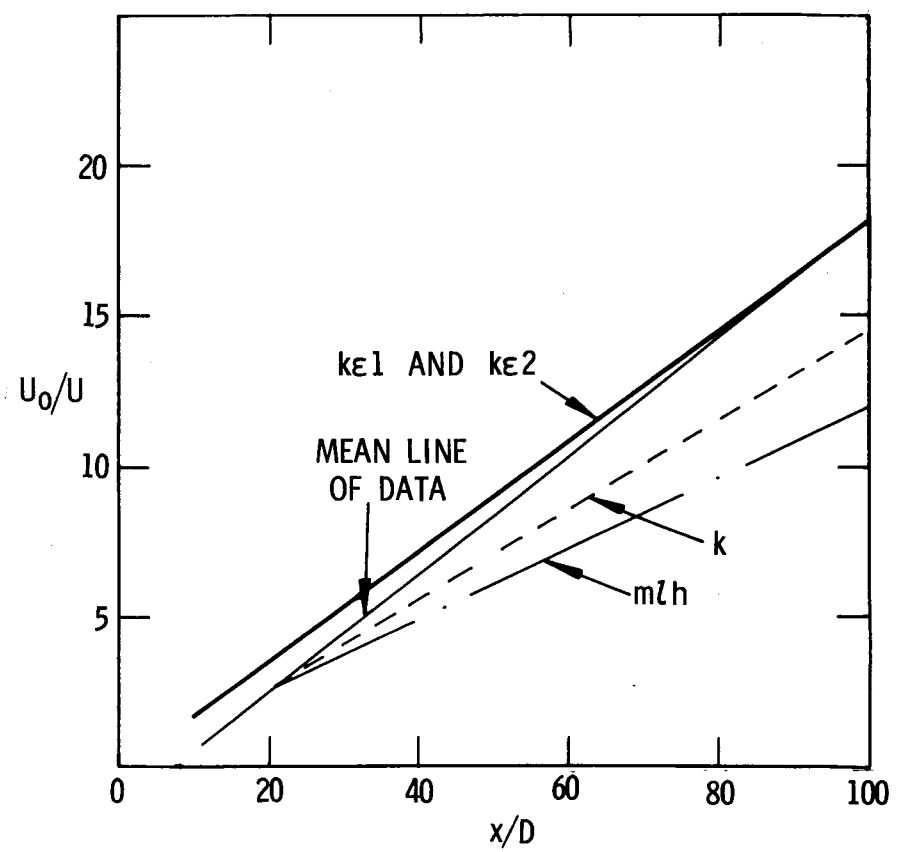
20
15
10
5
U0/U
kε1 AND kε2
MEAN LINE
OF DATA
k
mlh
0
20
40
60
80
100
x/D

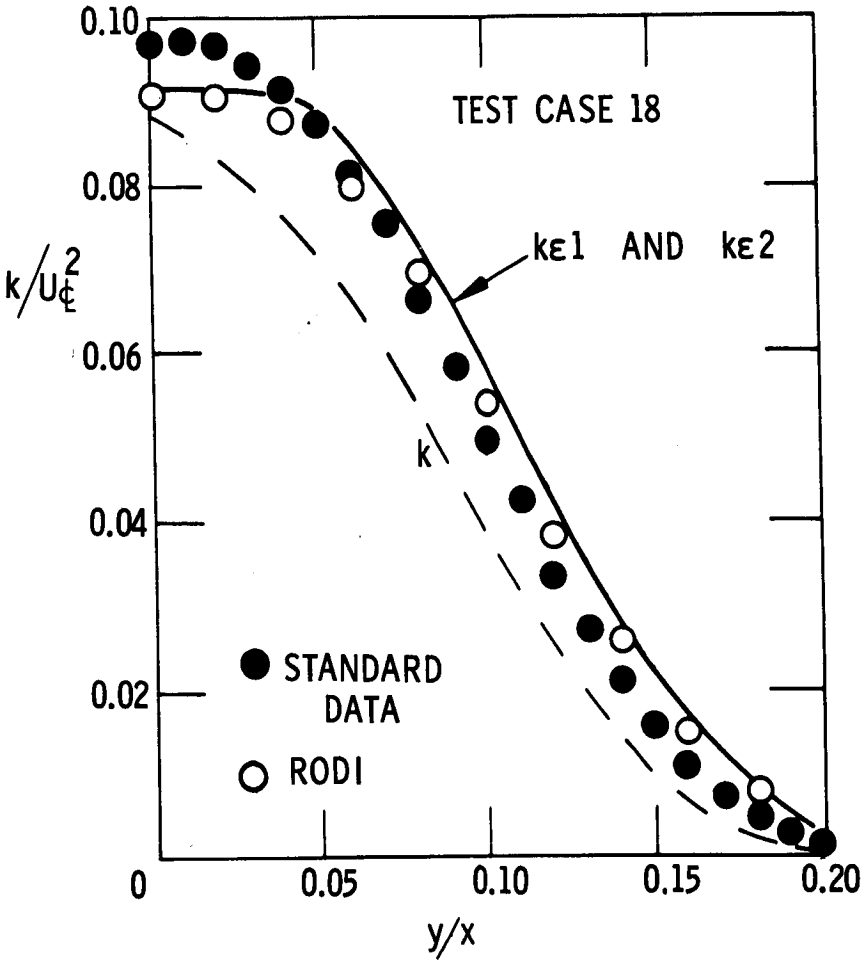
TEST CASE 18
kε1 AND kε2
k
STANDARD DATA
RODI
k/U_{ℓ}^2
y/x
0.10
0.08
0.06
0.04
0.02
0
0.05
0.10
0.15
0.20

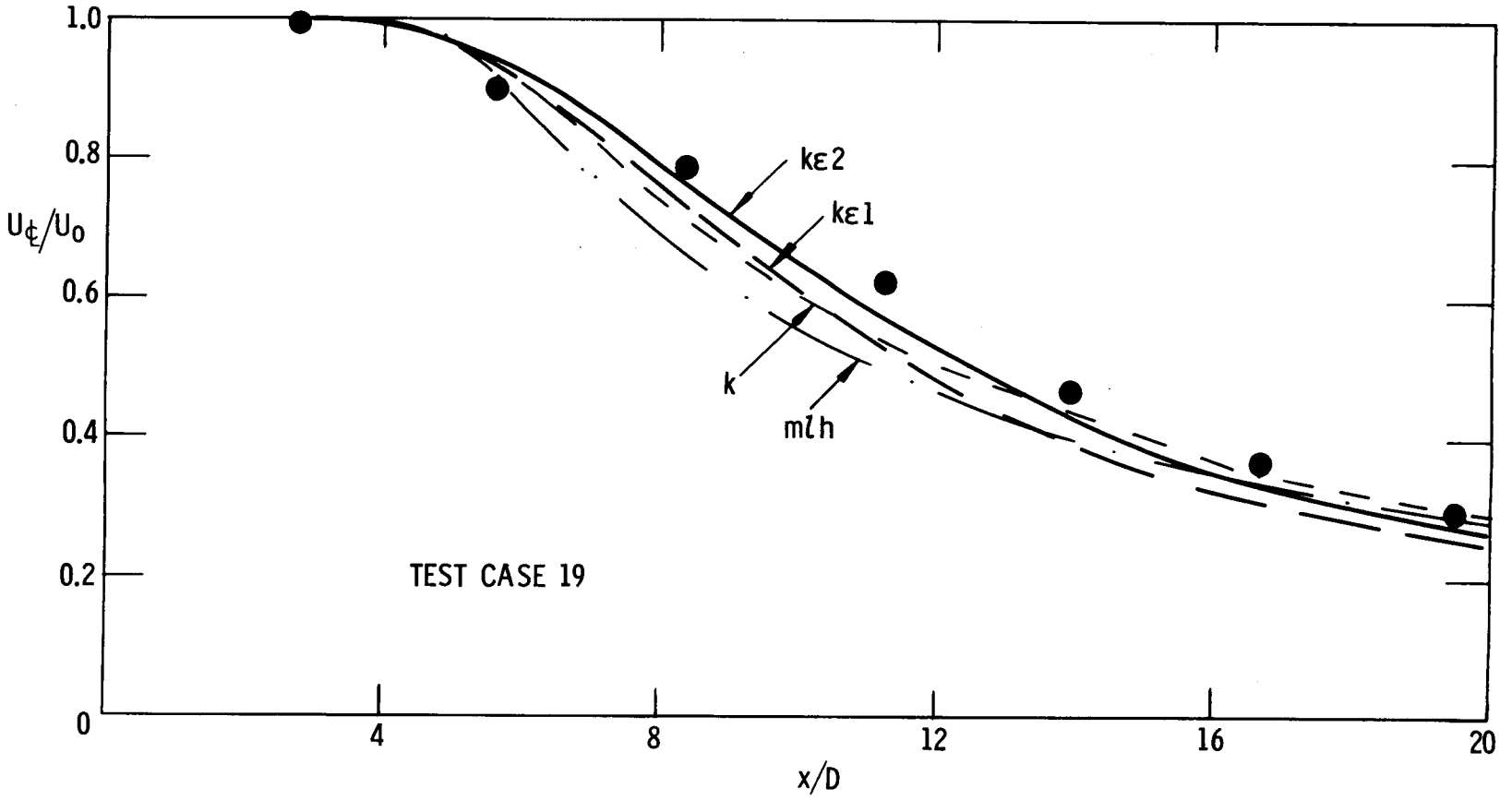
1.0
0.8
0.6
0.4
0.2
0
U_{ℓ}/U_0
kε2
kε1
k
mℓh
TEST CASE 19
4
8
12
16
20
x/D

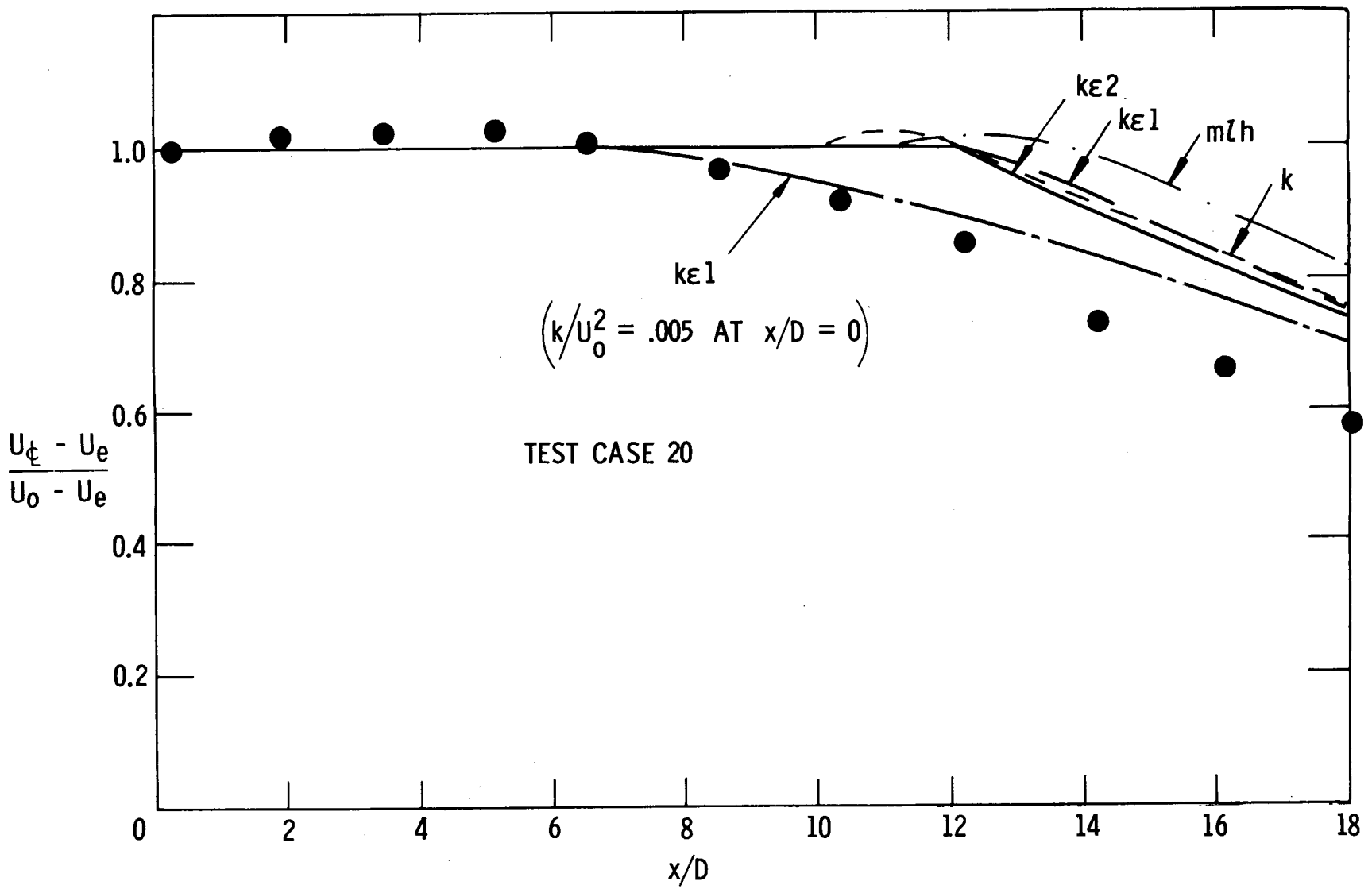
kε2
kε1
mlh
k
kε1
$\left(k/U_0^2 = .005 \text{ AT } x/D = 0\right)$
TEST CASE 20
$\frac{U_\ell - U_e}{U_0 - U_e}$
1.0
0.8
0.6
0.4
0.2
0
2
4
6
8
10
12
14
16
18
x/D

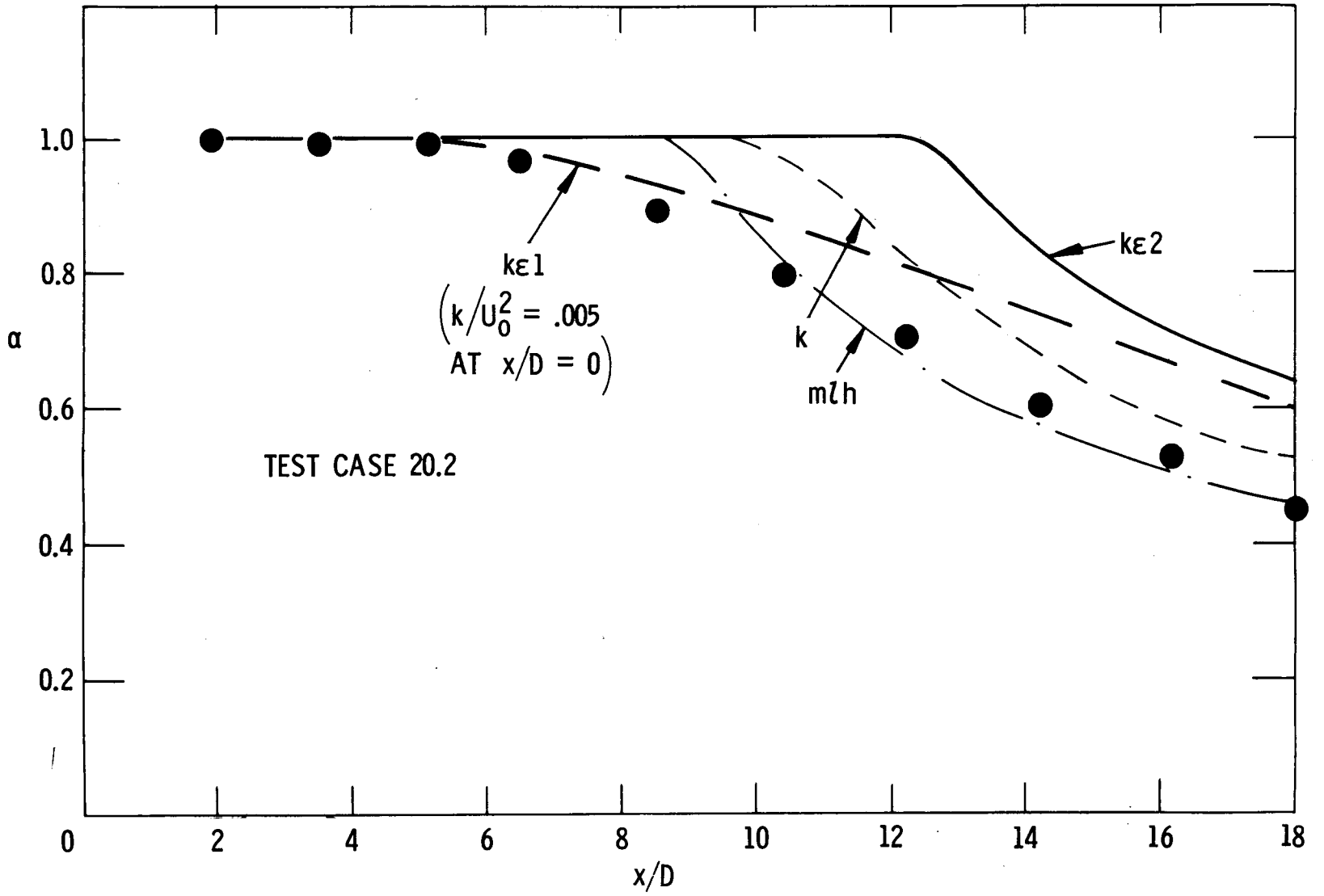
1.0
0.8
0.6
0.4
0.2
α
0
2
4
6
8
10
12
14
16
18
x/D
kε1
$(k/U_0^2 = .005$
AT x/D = 0)
kε2
k
mlh
TEST CASE 20.2

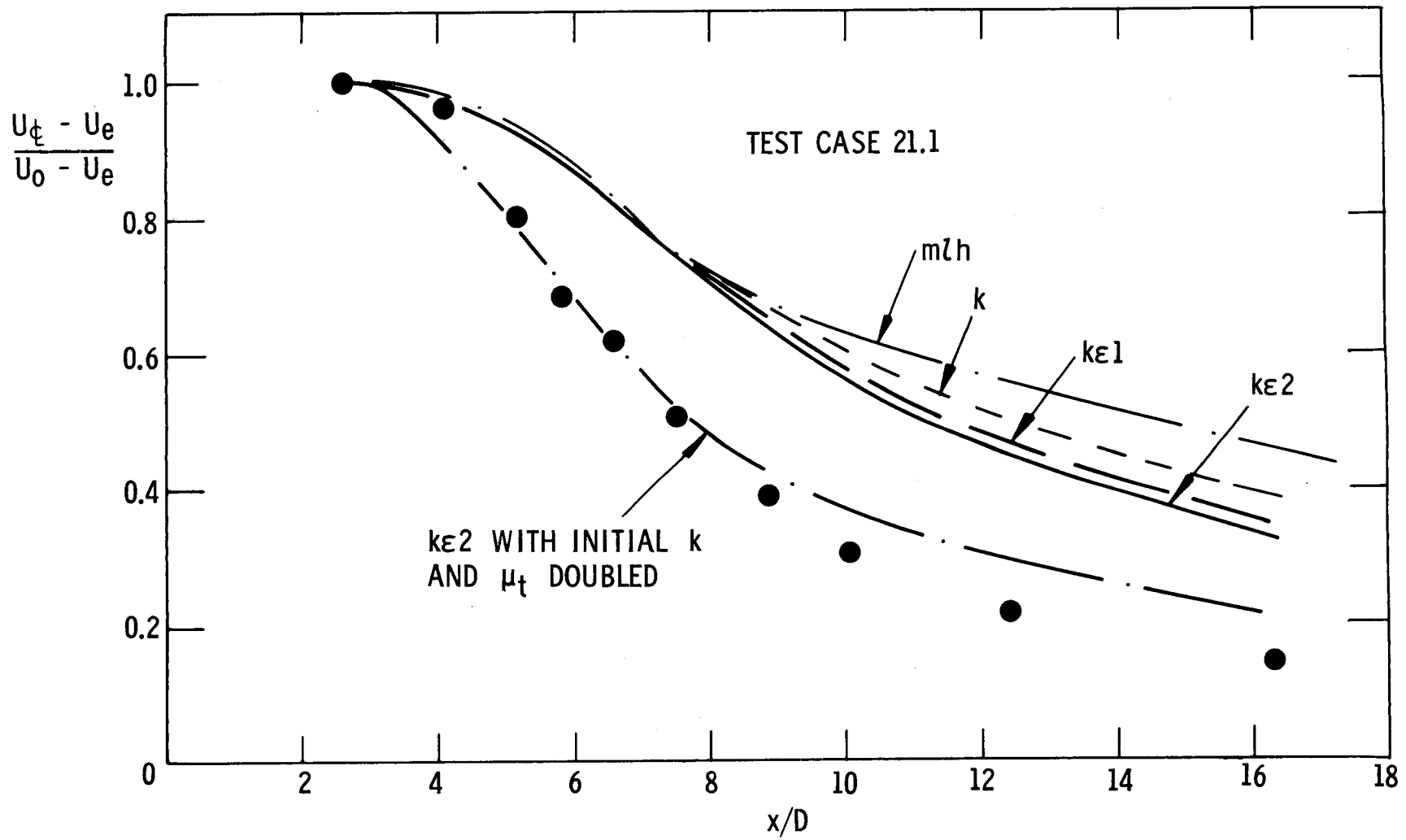
$\frac{U_{\ell} - U_e}{U_0 - U_e}$
1.0
0.8
0.6
0.4
0.2
0
2
4
6
8
10
12
14
16
18
x/D
TEST CASE 21.1
mℓh
k
kε1
kε2
kε2 WITH INITIAL k
AND μ_t DOUBLED

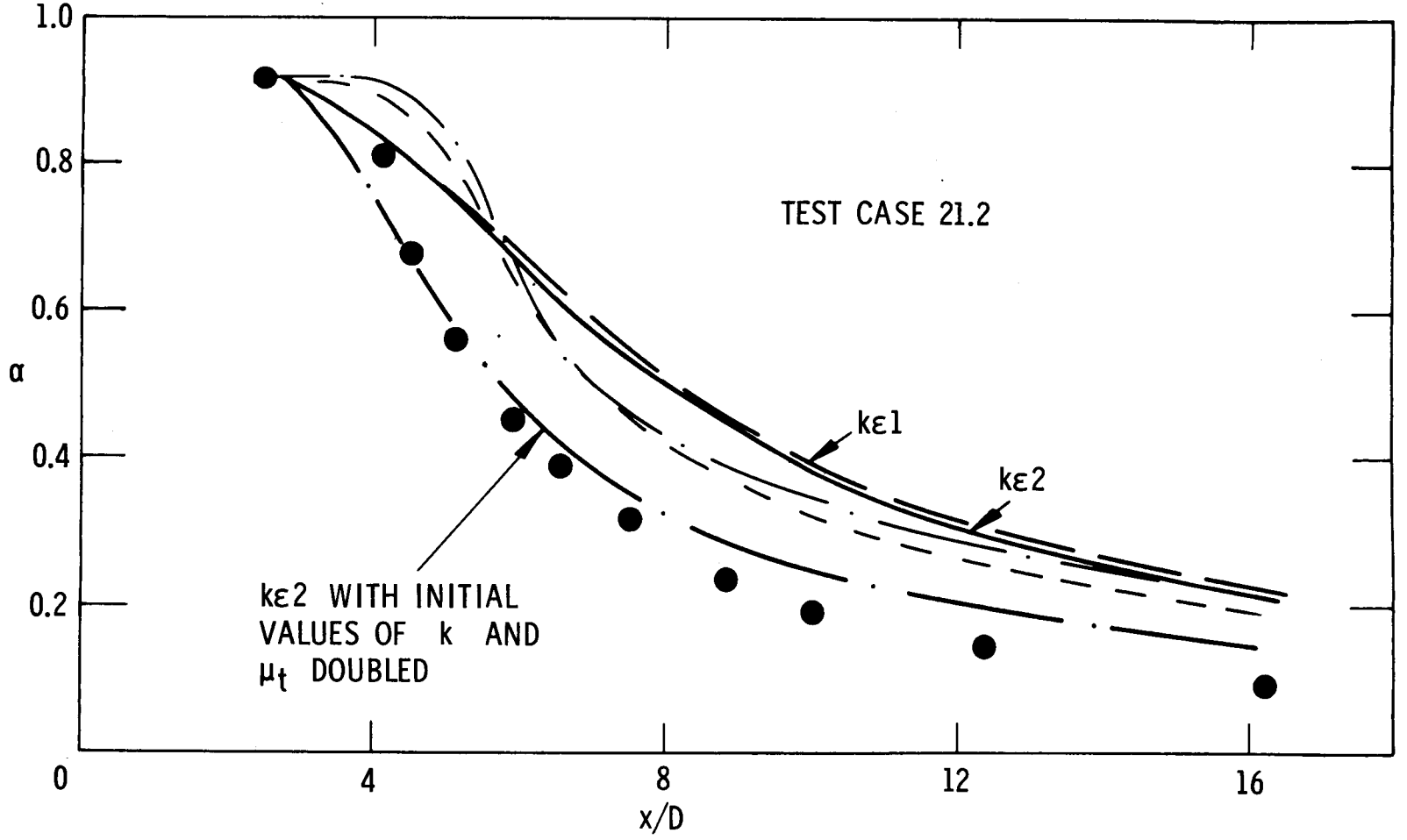
1.0
0.8
0.6
0.4
0.2
0
α
4
8
12
16
x/D
TEST CASE 21.2
kε1
kε2
kε2 WITH INITIAL VALUES OF k AND μt DOUBLED

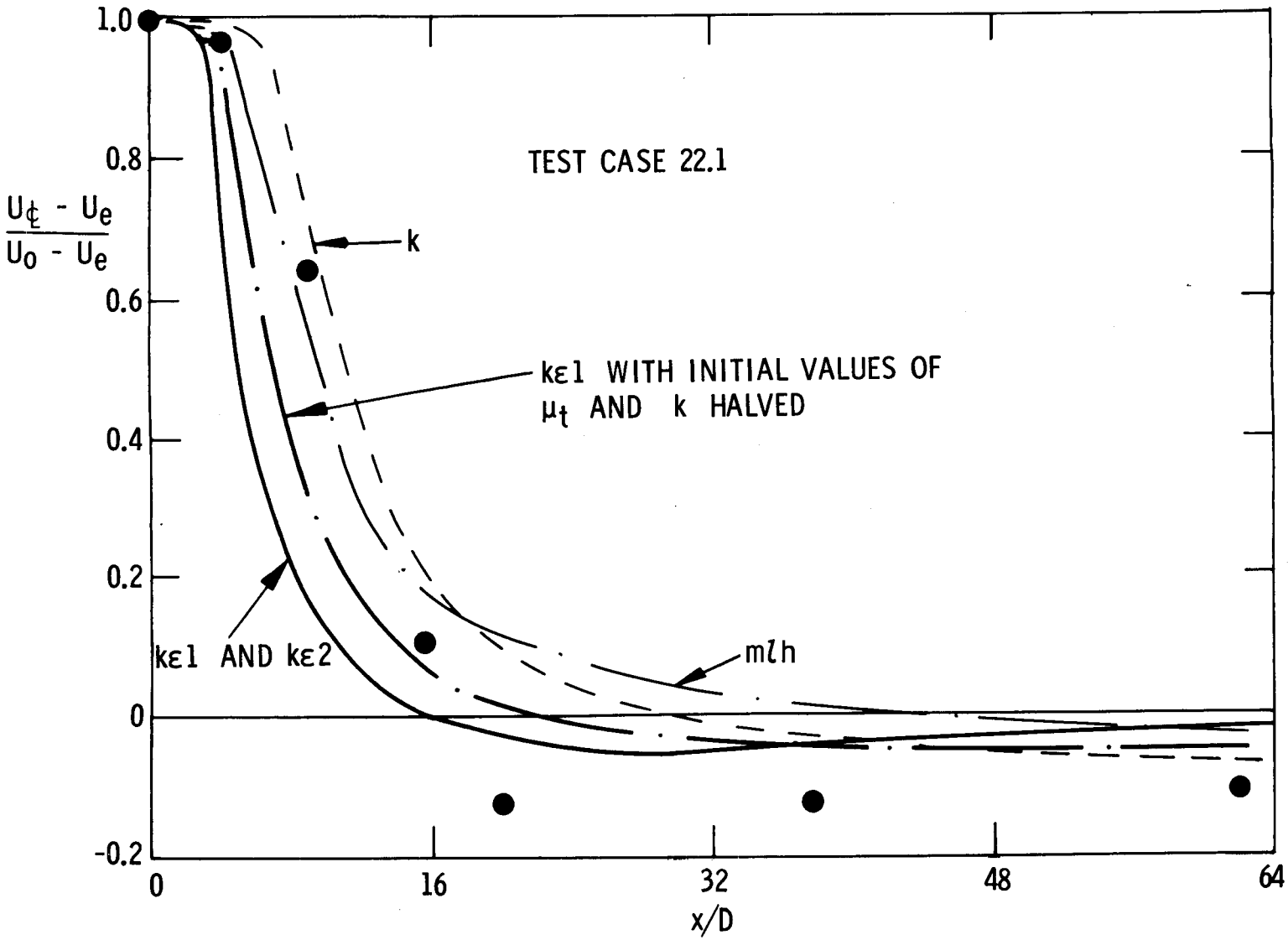
TEST CASE 22.1
$\frac{U_{\ell} - U_e}{U_0 - U_e}$
1.0
0.8
0.6
0.4
0.2
0
-0.2
0
16
32
48
64
x/D
k
kε1 WITH INITIAL VALUES OF
μ_t AND k HALVED
kε1 AND kε2
mlh

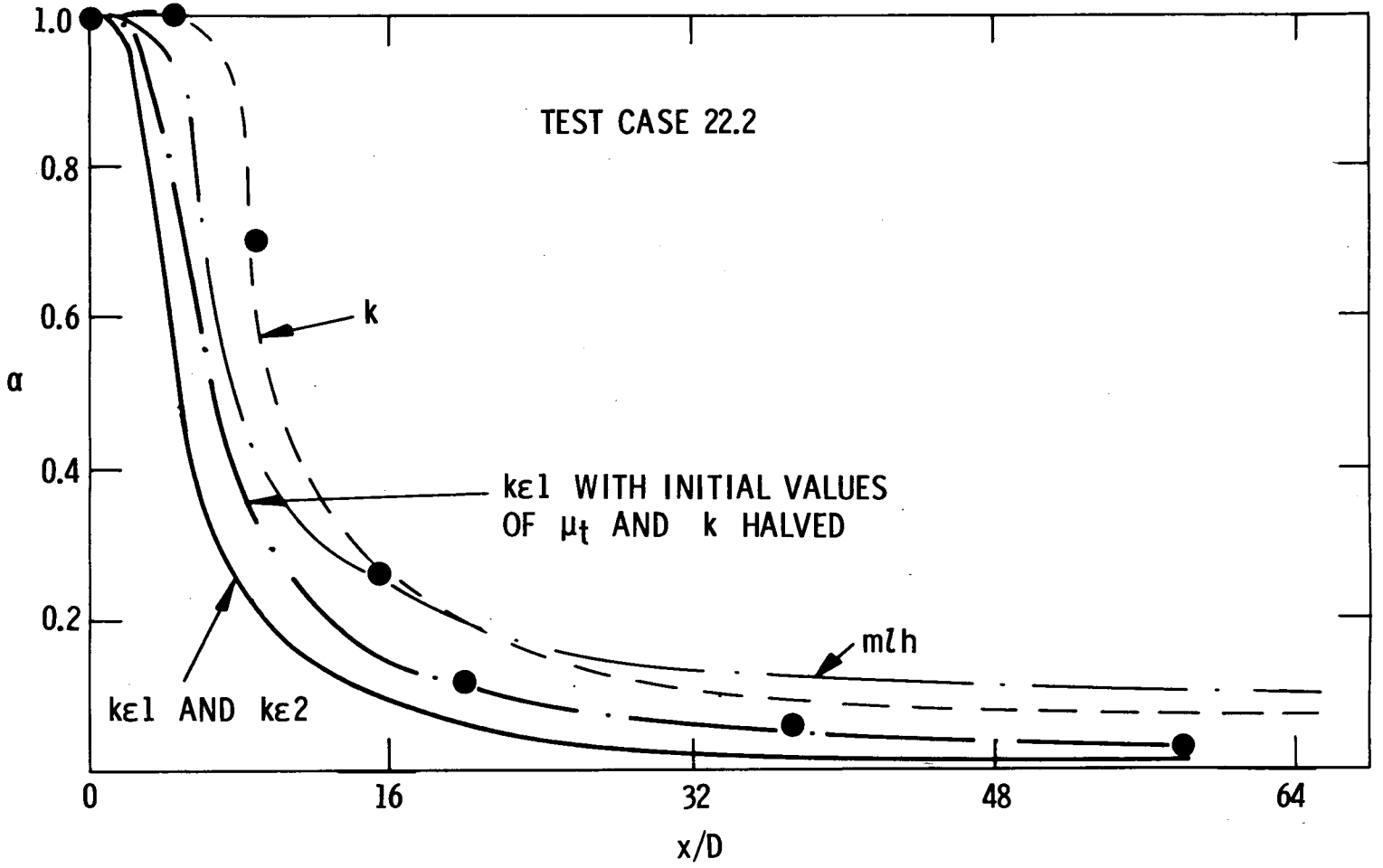
TEST CASE 22.2
1.0
0.8
0.6
0.4
0.2
α
k
kε1 WITH INITIAL VALUES
OF μt AND k HALVED
mlh
kε1 AND kε2
0
16
32
48
64
x/D

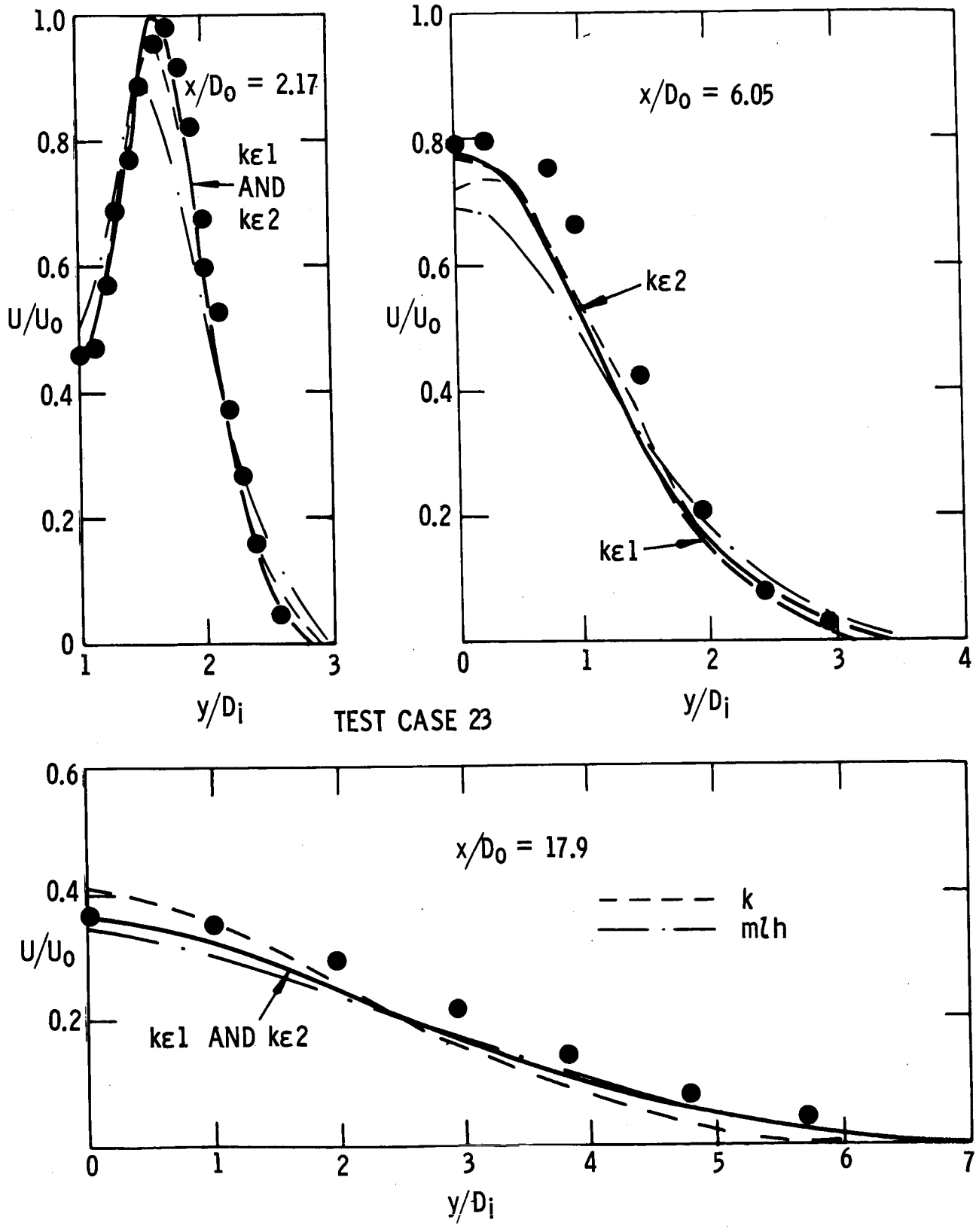
1.0
0.8
0.6
0.4
0.2
0
U/U0
x/D0 = 2.17
kε1
AND
kε2
1
2
3
y/Di
x/D0 = 6.05
kε2
kε1
0
1
2
3
4
y/Di
TEST CASE 23
0.6
0.4
0.2
U/U0
x/D0 = 17.9
k
mlh
kε1 AND kε2
0
1
2
3
4
5
6
7
y/Di

REFERENCES

1. Prandtl, L.: Bericht über Untersuchungen zur ausgebildeten Turbulenz. Z. Angew. Math. Mech., Bd. 5, Heft 2, Apr. 1925, pp. 136-139.

2. Prandtl, L.: Über ein neues Formelsystem für die ausgebildete Turbulenz. Nachr. Akad. Wiss. Göttingen. Math.-Physik. Kl., 1945, pp. 6-19.

3. Harlow, Francis H.; and Nakayama, Paul I.: Transport of Turbulence Energy Decay Rate. LA-3854 (Contract W-7405-ENG. 36), Los Alamos Sci. Lab., Univ. of California, Feb. 20, 1968.

4. Jones, W. P.; and Launder, B. E.: The Prediction of Laminarization With a Two-Equation Model of Turbulence. Int. J. Heat & Mass Transfer, vol. 15, no. 2, Feb. 1972, pp. 301-314.

5. Rodi, W.; and Spalding, D. B.: A Two-Parameter Model of Turbulence, and Its Application to Free Jets. Wärme- und Stoffübertragung, vol. 3, no. 2, 1970, pp. 85-95.

6. Ng, K. H.; and Spalding, D. B.: Turbulence Model for Boundary Layers Near Walls. Phys. Fluids, vol. 15, no. 1, Jan. 1972, pp. 20-30.

7. Spalding, D. B.: The kW Model of Turbulence. TM/TN/A/16, Dep. Mech. Eng., Imp. Coll. Sci. & Technol., Aug. 1971.

8. Rodi, Wolfgang: The Prediction of Free Turbulent Boundary Layers by Use of a Two-Equation Model of Turbulence. Ph. D. Thesis, Univ. of London, 1972.

9. Hanjalić, K.; and Launder, B. E.: A Reynolds Stress Model of Turbulence and Its Application to Thin Shear Flows. J. Fluid Mech., vol. 52, pt. 4, Apr. 25, 1972, pp. 609-638.

10. Rotta, J.: Statistical Theory of Nonhomogeneous Turbulence. Part I: Z. Physik, Bd. 129, 1951, pp. 547-572.

11. Patankar, S. V.; and Spalding, D. B.: Heat and Mass Transfer in Boundary Layers. Second ed., Int. Textbook Co. Ltd. (London), c.1970.

12. Mellor, George L.; and Herring, H. James: Two Methods of Calculating Turbulent Boundary Layer Behavior Based on Numerical Solutions of the Equations of Motion. Computation of Turbulent Boundary Layers – 1968 AFOSR-IFP-Stanford Conference, Vol. I, S. J. Kline, M. V. Morkovin, G. Sovran, and D. J. Cockrell, eds., Stanford Univ., c.1969, pp. 331-345.

13. Naot, D.; Shavit, A.; and Wolfshtein, M.: Interactions Between Components of the Turbulent Velocity Correlation Tensor Due to Pressure Fluctuations. Israel J. Technol., vol. 8, no. 3, 1970, pp. 259-269.

14. Reynolds, W. C.: Computation of Turbulent Flows – State-of-the-Art, 1970. Rep. MD-27 (Grants NSF-GK-10034 and NASA-NgR-05-020-420), Dep. Mech. Eng., Stanford Univ., Oct. 1970. (Available as NASA CR-128372.)

15. Rodi, W.: A New Method of Analysing Hot-Wire Signals in Highly Turbulent Flow, and Its Evaluation in a Round Jet. ET/TN/B/10, Dep. Mech. Eng., Imp. Coll. Sci. & Technol., Aug. 1971.

16. Bradshaw, P.; Ferriss, D. H.; and Johnson, R. F.: Turbulence in the Noise-Producing Region of a Circular Jet. J. Fluid Mech., vol. 19, pt. 4, Aug. 1964, pp. 591-624.

17. Bradbury, L. J. S.: The Structure of a Self-Preserving Turbulent Plane Jet. J. Fluid Mech., vol. 23, pt. 1, Sept. 1965, pp. 31-64.

18. Klebanoff, P. S.: Characteristics of Turbulence in a Boundary Layer With Zero Pressure Gradient. NACA Rep. 1247, 1955. (Supersedes NACA TN 3178.)

19. Champagne, F. H.; and Wygnanski, I. J.: An Experimental Investigation of Coaxial Turbulent Jets. Int. J. Heat & Mass Transfer, vol. 14, no. 9, Sept. 1971, pp. 1445-1464.

TABLE 1.- THE MIXING-LENGTH HYPOTHESIS ($m\ell h$)

$$-\overline{uv} = \ell_m^2 \left|\frac{\partial U}{\partial y}\right| \left(\frac{\partial U}{\partial y}\right)$$

where

$$\ell_m = \lambda y_G$$

and

$\lambda = 0.11$ (Axisymmetric flows)

$= 0.125$ (Plane flows)

For a monotonically increasing/decreasing velocity profile, the characteristic shear width of the flow is defined by

$$y_G = y_2 - y_1$$

where at y_1

$$\frac{U - U_I}{U_E - U_I} = 0.1$$

and at y_2

$$\frac{U - U_I}{U_E - U_I} = 0.9$$

(U_I = Axial velocity at internal boundary; U_E = Axial velocity at external boundary)

For velocity profiles without a maximum or minimum at either boundary:

At y_1

$$\frac{U - U_I}{\overline{U} - U_I} = 0.1$$

(For inner region of flow, i.e., between the internal boundary and the point of occurrence of the minimum/maximum velocity $\overline{U}$)

or at y_1

$$\frac{U - \overline{U}}{U_E - \overline{U}} = 0.9$$

(For outer region of flow)

At y_2

$$U = \overline{U}$$

For diffusion of enthalpy and species,

$$\sigma_h = \sigma_m = 0.5$$

TABLE 2.- THE PRANDTL ENERGY MODEL (k)

$$-\overline{uv} = C_\mu k^{1/2} l \left(\frac{\partial U}{\partial y}\right)$$

where

$$l = \lambda_s y_G \qquad \left(\text{With } y_G \text{ determined as in table 1}\right)$$

and

$\lambda_s = 0.625$ (Axisymmetric flows)

$= 0.875$ (Plane flows)

Equation solved for conservation of kinetic energy of turbulence is

$$\rho \frac{Dk}{Dt} = \frac{1}{y^j} \frac{\partial}{\partial y}\left(y^j \frac{\mu_t}{\sigma_k} \frac{\partial k}{\partial y}\right) + \mu_t \left(\frac{\partial U}{\partial y}\right)^2 - \frac{\rho k^{3/2}}{l}$$

where

$C_\mu = 0.08$

$\sigma_k = 0.7$

For diffusion of enthalpy and species,

$\sigma_h = \sigma_m = 0.5$

TABLE 3.- THE ENERGY-DISSIPATION MODEL (kϵ1)

$$-\rho\overline{uv} = \mu_t \frac{\partial U}{\partial y}$$

where

$$\mu_t = C_\mu \rho \frac{k^2}{\epsilon}$$

$$\rho \frac{Dk}{Dt} = \frac{1}{y^j} \frac{\partial}{\partial y}\left(y^j \frac{\mu_t}{\sigma_k} \frac{\partial k}{\partial y}\right) + \mu_t \left(\frac{\partial U}{\partial y}\right)^2 - \rho\epsilon$$

$$\rho \frac{D\epsilon}{Dt} = \frac{1}{y^j} \frac{\partial}{\partial y}\left(y^j \frac{\mu_t}{\sigma_\epsilon} \frac{\partial \epsilon}{\partial y}\right) + C_{\epsilon 1} \frac{\epsilon}{k} \mu_t \left(\frac{\partial U}{\partial y}\right)^2 - C_{\epsilon 2} \frac{\rho \epsilon^2}{k}$$

For plane flows:

C_μ	$C_{\epsilon 2}$	$C_{\epsilon 1}$	σ_k	σ_ϵ
0.09	1.92	1.43	1.0	1.3

For axisymmetric flows:

The same as plane flows except

$$C_\mu = 0.09 - 0.04f$$

$$C_{\epsilon 2} = 1.92 - 0.0667f$$

where

$$f \equiv \left| \frac{y_G}{2\,\Delta U}\left(\frac{dU_\mathcal{L}}{dx} - \left|\frac{dU_\mathcal{L}}{dx}\right|\right)\right|^{0.2}$$

For diffusion of enthalpy and species,

$$\sigma_m = \sigma_h = 0.7$$

TABLE 4.- THE EXTENDED ENERGY-DISSIPATION MODEL ($k\epsilon 2$)

The data are the same as in table 3 except as noted below.

For plane flows:

C_μ	$C_{\epsilon 2}$	$C_{\epsilon 1}$	σ_k	σ_ϵ
*	1.94	1.40	1.0	1.3

$$^{*}\, C_\mu = 0.09 g\left(\overline{P/\epsilon}\right)$$

where

$$\left(\overline{P/\epsilon}\right) \equiv \frac{\int_{y_1}^{y_2} \rho\overline{uv}\left(\frac{P}{\epsilon}\right) y^j dy}{\int_{y_2}^{y_1} \rho\overline{uv} y^j dy}$$

and the function $g\left(\overline{P/\epsilon}\right)$ is shown in figure 1

For axisymmetric flows:

The same as plane flows except

$$C_\mu = 0.09 g\left(\overline{P/\epsilon}\right) - 0.0534f$$

$$C_{\epsilon 2} = 1.94 - 0.1336f$$

TABLE 5.- THE HANJALIĆ-LAUNDER $\overline{uv}k\epsilon$ MODEL

The Reynolds shear stress $-\rho\overline{uv}$ is found from

$$\frac{D\overline{uv}}{Dt} = C_s \frac{\partial}{\partial y}\left(\frac{k^2}{\epsilon}\frac{\partial \overline{uv}}{\partial y}\right) - C_{\phi 1}\left(\frac{\overline{uv}\epsilon}{k} + C_\mu\, k \frac{\partial U}{\partial y}\right)$$

$$\frac{Dk}{Dt} = 0.9C_s \frac{\partial}{\partial y}\left(\frac{k^2}{\epsilon}\frac{\partial \overline{uv}}{\partial y}\right) - \overline{uv}\frac{\partial U}{\partial y} - \epsilon$$

$$\frac{D\epsilon}{Dt} = C_\epsilon \frac{\partial}{\partial y}\left(\frac{k^2}{\epsilon}\frac{\partial \epsilon}{\partial y}\right) - C_{\epsilon 1}\frac{\overline{uv}\epsilon}{k}\frac{\partial U}{\partial y} - C_{\epsilon 2}\frac{\epsilon^2}{k}$$

where

C_s	$C_{\phi 1}$	C_μ	C_ϵ	$C_{\epsilon 1}$	$C_{\epsilon 2}$
0.1	2.8	0.09	0.07	1.40	1.95

TABLE 6.- REYNOLDS STRESS MODELS $\left(\overline{u_i u_j}\epsilon\right)$

Reynolds stresses $-\rho\overline{u_i u_j}$ calculated from

$$\frac{D\overline{u_i u_j}}{Dt} = D_{ij} + \Phi_{ij} - \underbrace{\left(\overline{u_i u_\ell}\frac{\partial U_j}{\partial x_\ell} + \overline{u_j u_\ell}\frac{\partial U_i}{\partial x_\ell}\right)}_{P_{ij}} - \frac{2}{3}\epsilon\delta_{ij}$$

1. Simple version for D_{ij}

$$D_{ij} = C_s\frac{\partial}{\partial x_k}\left(\frac{k}{\epsilon}\overline{u_k u_\ell}\frac{\partial\overline{u_i u_j}}{\partial x_\ell}\right)$$

$C_s = 0.25$

2. Tensor invariant D_{ij}

$$D_{ij} = C_s\frac{\partial}{\partial x_k}\frac{k}{\epsilon}\left(\overline{u_i u_\ell}\frac{\partial\overline{u_j u_k}}{\partial x_\ell} + \overline{u_j u_\ell}\frac{\partial\overline{u_k u_i}}{\partial x_\ell} + \overline{u_k u_\ell}\frac{\partial\overline{u_i u_j}}{\partial x_\ell}\right)$$

$C_s = 0.10$

A. Rotta-Wolfshtein-Reynolds, Φ_{ij}

$$-C_{\phi1}\frac{\epsilon}{k}\left(\overline{u_i u_j} - \frac{2}{3}\delta_{ij}k\right) - C_{\phi2}\left(P_{ij} - \frac{2}{3}\delta_{ij}P\right)$$

$C_{\phi1} = 2.8$ $\quad C_{\phi2} = 0.4$ $\quad P$ = Total production rate of k

B. Rotta-Hanjalić-Launder, Φ_{ij}

$$-C_{\phi1}\frac{\epsilon}{k}\left(\overline{u_i u_j} - \frac{2}{3}\delta_{ij}k\right) + \left(\phi_{ij} + \phi_{ji}\right)$$

where

$$\phi_{ij} \equiv \frac{\partial U_l}{\partial x_m}a_{\ell j}^{mi}$$

$$a_{\ell j}^{mi} = \alpha\overline{u_m u_i}\delta_{ij} + \beta\left(\overline{u_m u_\ell}\delta_{ij} + \overline{u_m u_j}\delta_{\ell i} + \overline{u_i u_j}\delta_{m\ell} + \overline{u_i u_\ell}\delta_{mj}\right) + \left[\gamma\delta_{mi}\delta_{\ell j} + \eta\left(\delta_{m\ell}\delta_{ij} + \delta_{mj}\delta_{i\ell}\right)\right]k$$

$$+ \frac{\nu\left(\overline{u_m u_j u_i u_\ell} + \overline{u_m u_\ell u_i u_j}\right)}{k} + C_{\phi2}\frac{\left(\overline{u_m u_i u_\ell u_j}\right)}{k}$$

$\alpha = \dfrac{10 - 8C_{\phi2}}{11}$ $\quad \beta = \dfrac{-(2 - 6C_{\phi2})}{11}$ $\quad \gamma = \dfrac{-(4 - 12C_{\phi2})}{55}$ $\quad \eta = \dfrac{6 - 18C_{\phi2}}{55}$

$\nu = -C_{\phi2}$ $\quad C_{\phi1} = 2.5$ $\quad C_{\phi2} = 0.3$

C. Rotta-Launder, Φ_{ij} (present work)

$$-C_{\phi1}\frac{\epsilon}{k}\left(\overline{u_i u_j} - \frac{2}{3}\delta_{ij}k\right) + \left(\phi_{ij} + \phi_{ji}\right)$$

where

$$\phi_{ij} \equiv \frac{\partial U_l}{\partial x_m}a_{\ell j}^{mi}$$

$$a_{\ell j}^{mi} = \alpha\delta_{mi}\overline{u_\ell u_j} + \beta\left(\delta_{m\ell}\overline{u_i u_j} + \delta_{mj}\overline{u_i u_\ell} + \delta_{i\ell}\overline{u_m u_j} + \delta_{ij}\overline{u_m u_\ell}\right) + \gamma\delta_{\ell j}\overline{u_m u_i} + \left[\eta\delta_{mi}\delta_{\ell j} + \nu\left(\delta_{m\ell}\delta_{ij} + \delta_{mj}\delta_{i\ell}\right)\right]k$$

$\beta = \dfrac{-(2 + 3\alpha)}{11}$ $\quad \gamma = \dfrac{4\alpha + 10}{11}$ $\quad \eta = \dfrac{-(50\alpha + 4)}{55}$ $\quad \nu = \dfrac{20\alpha + 6}{55}$ $\quad \alpha = 0.3$ $\quad C_{\phi1} = 1.5$

$$\frac{D\epsilon}{Dt} = C_\epsilon\frac{\partial}{\partial x_k}\left(\frac{k}{\epsilon}\overline{u_k u_\ell}\frac{\partial\epsilon}{\partial x_\ell}\right) - C_{\epsilon1}\frac{\overline{u_i u_j}\epsilon}{k}\frac{\partial U_i}{\partial x_j} - C_{\epsilon2}\frac{\epsilon^2}{k}$$

$C_\epsilon = 0.2$ $\quad C_{\epsilon1} = 1.43$ $\quad C_{\epsilon2} = 1.92$ (Versions A and B for Φ_{ij})

$C_\epsilon = 0.16$ $\quad C_{\epsilon1} = 1.50$ $\quad C_{\epsilon2} = 1.95$ (Version C for Φ_{ij})

TABLE 7.- INITIAL CONDITIONS

Test case	$\frac{\mu_t}{\rho D \Delta U}$	ρ at –	Remarks
1, 2, 3			Arbitrary initial conditions
4			$\overline{uv}$ given; $k = \frac{\lvert\overline{uv}\rvert}{0.3}$; $\overline{u^2}/k$, $\overline{v^2}/k$, $\overline{w^2}/k$ as in test case 14
5	3.68×10^{-3}	e	D taken as 2.54 cm
6			$\overline{uv}$ and k taken from reference 16
7	3.3×10^{-3}	l	
8	6.6×10^{-3}	l	
9	1.6×10^{-3}	l	
10	0.72×10^{-3}	e	
11	1.25×10^{-3}	e	g = 0.8
12	5.5×10^{-3}	l	
13			$\overline{uv}$ and k from self-preserving plane jet (ref. 17); $\overline{u^2}/k$, $\overline{v^2}/k$, $\overline{w^2}/k$ assumed to be 2/3
14			$\overline{uv}$ given; $\overline{u^2}$ and $\overline{v^2}$ from reference paper for test case 14; $\overline{w^2}$ from reference 18; g = 1.2
15			$\overline{uv}$ given; k from reference paper for test case 15; computations begun at second station
16	0.19×10^{-3}	l	
17	12.9×10^{-3}		g = 1.3
18			A continuation of case 6
19	5×10^{-3}	l	
20	0.5×10^{-3}	e	
21	2.3×10^{-3}	e	
22	27×10^{-3}	l	
23			$\overline{u^2}$ and $\overline{v^2}$ given; $\overline{w^2} = \overline{v^2}$ assumed; $\overline{uv}$ from reference 19; g = 0.8; computations begun at second station

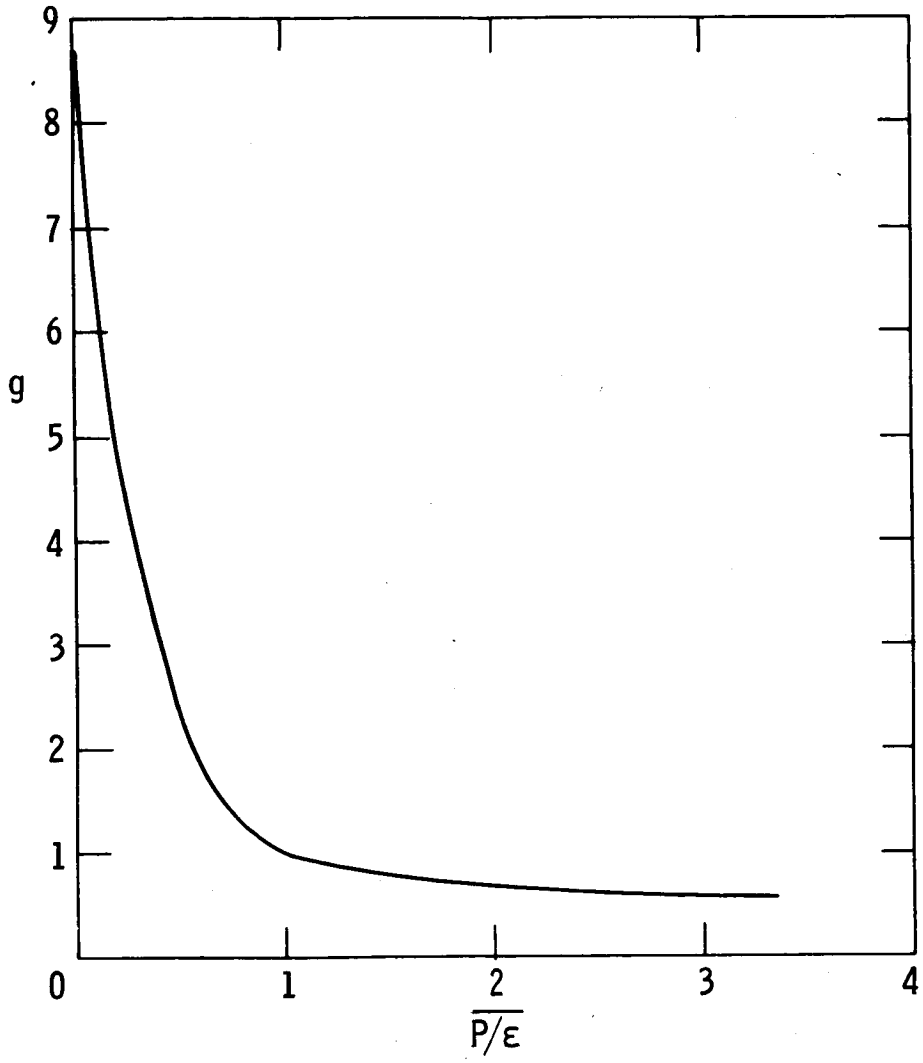

Figure 1.- Variation of g with $\overline{P/\epsilon}$ for kϵ2 model.

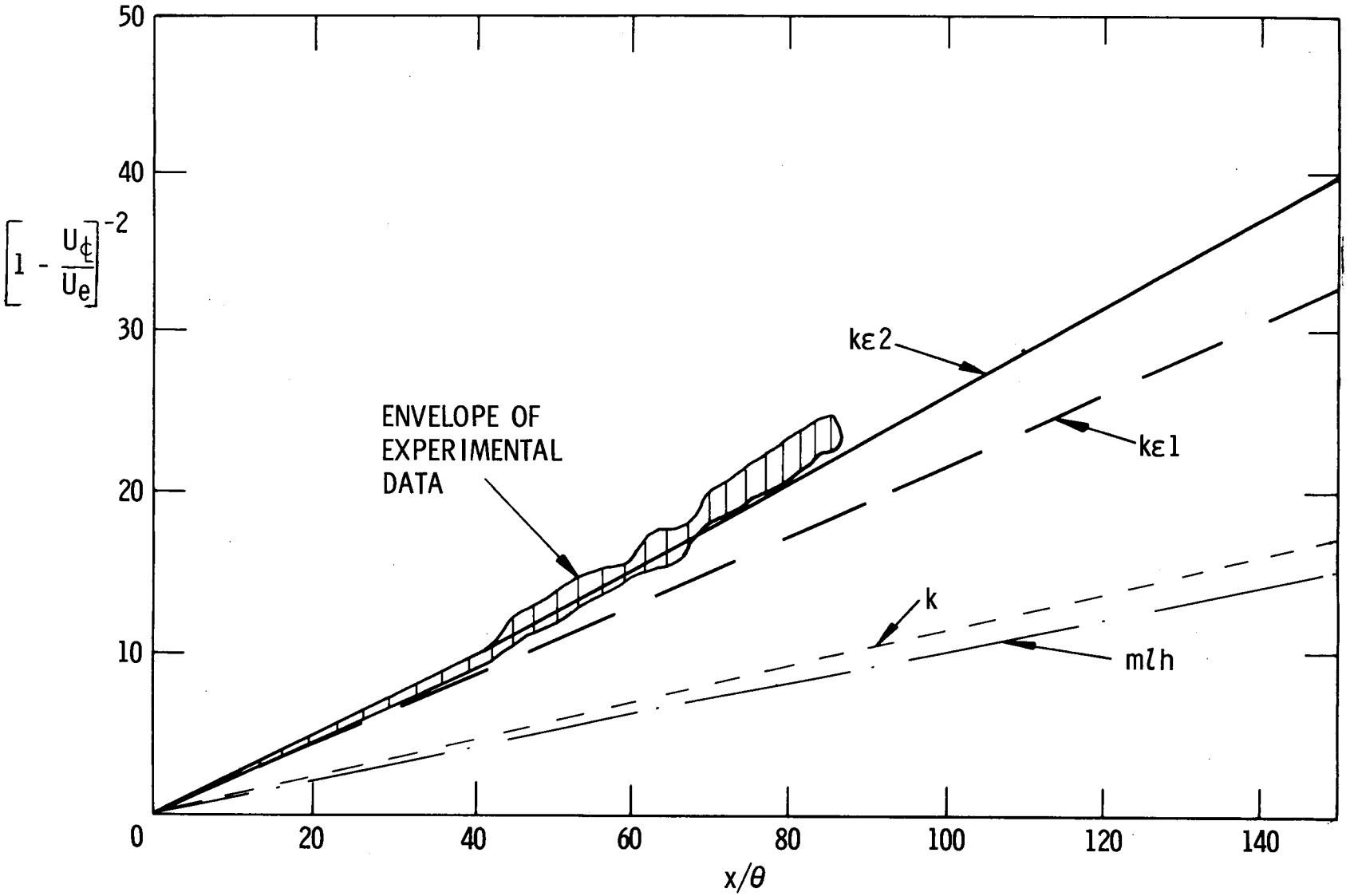

Figure 2.- Variation of $\left[1 - \frac{U_{C_L}}{U_e}\right]^{-2}$ with x/θ for case 13.

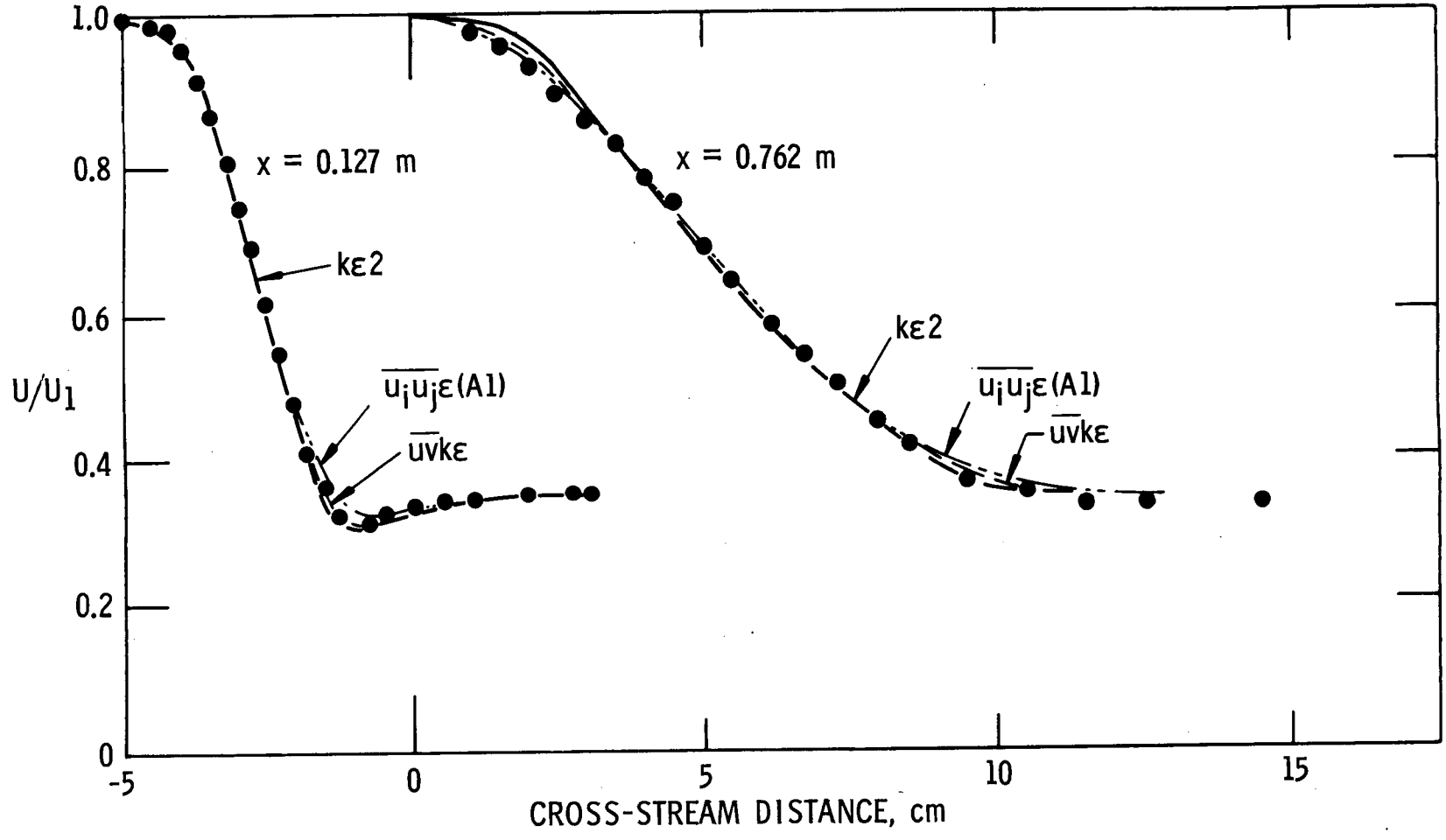

(a) Velocity profiles.

Figure 3.- Stress models, case 4. (Letter and number in parentheses denote modeling practice; see table 6.)

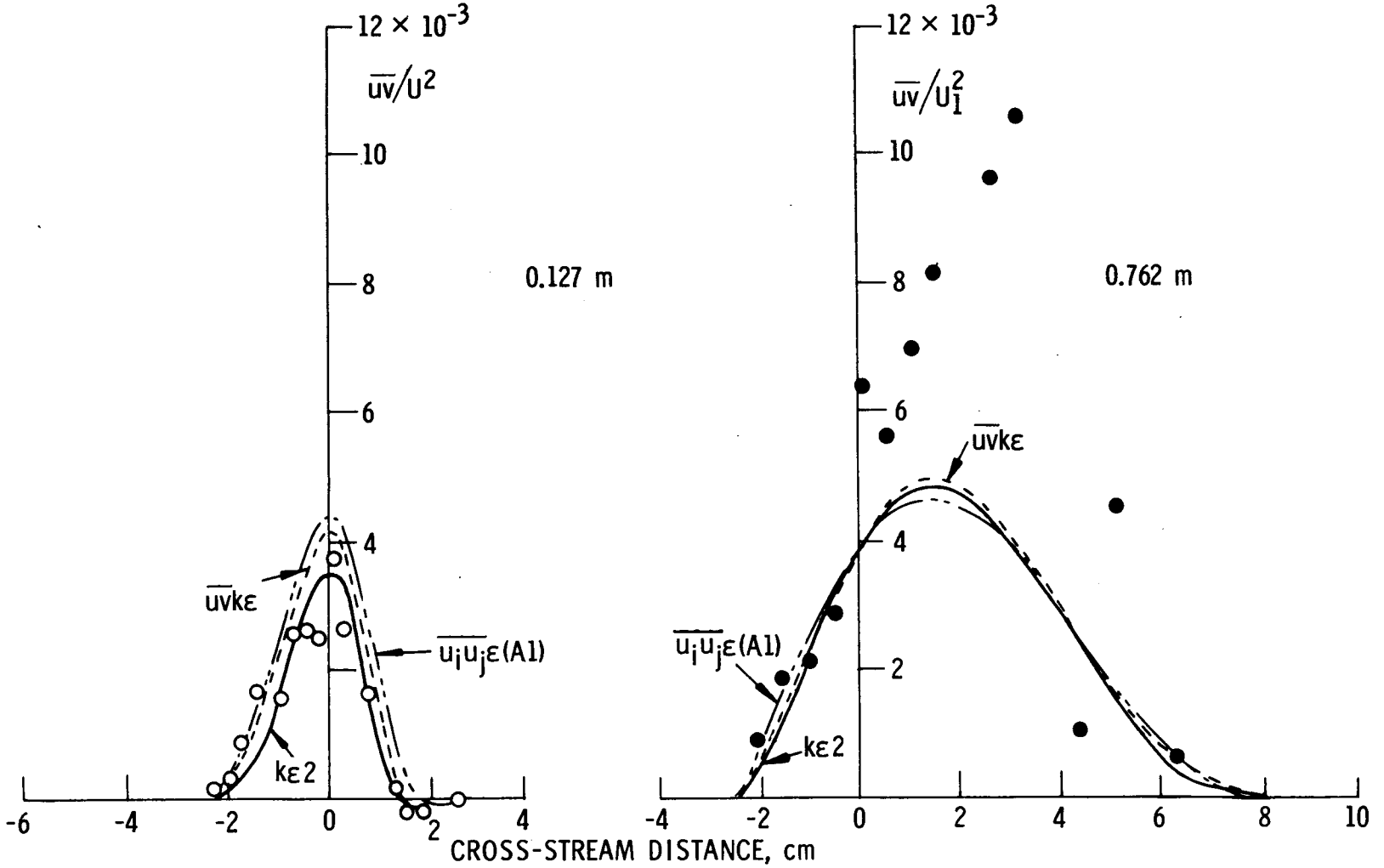

(b) Shear-stress profiles.

Figure 3.- Concluded.

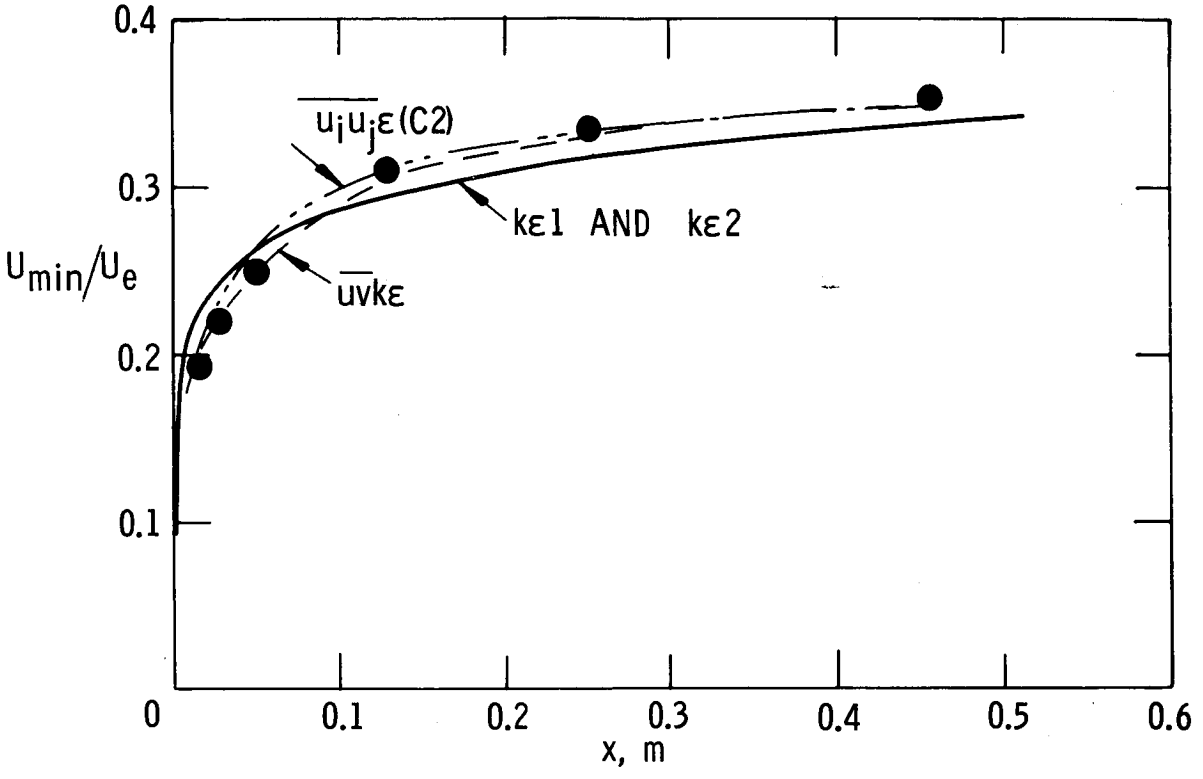

Figure 4.- Variation of minimum velocity for case 4.

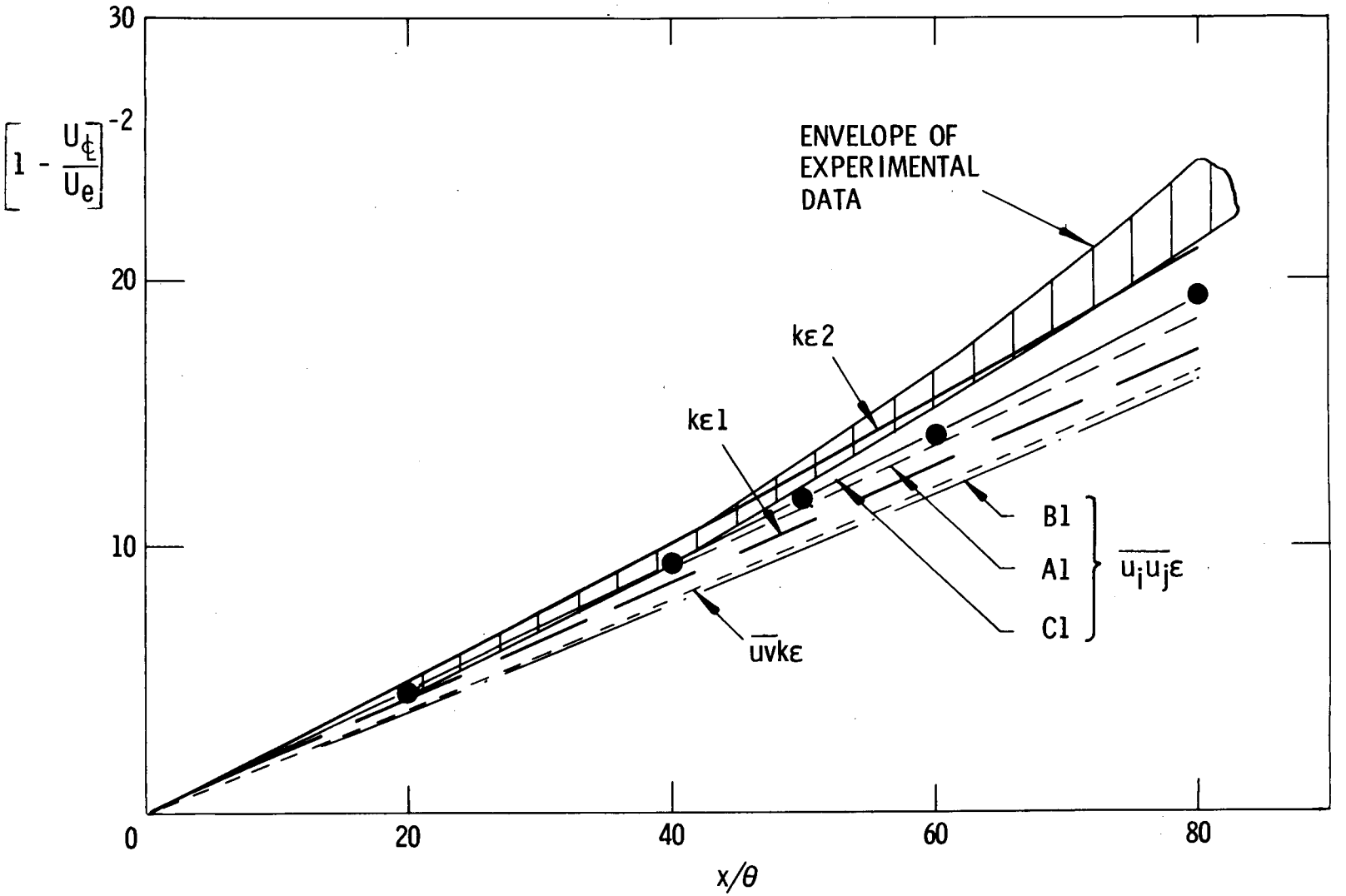

Figure 5.- Decay of plane jet in moving stream.

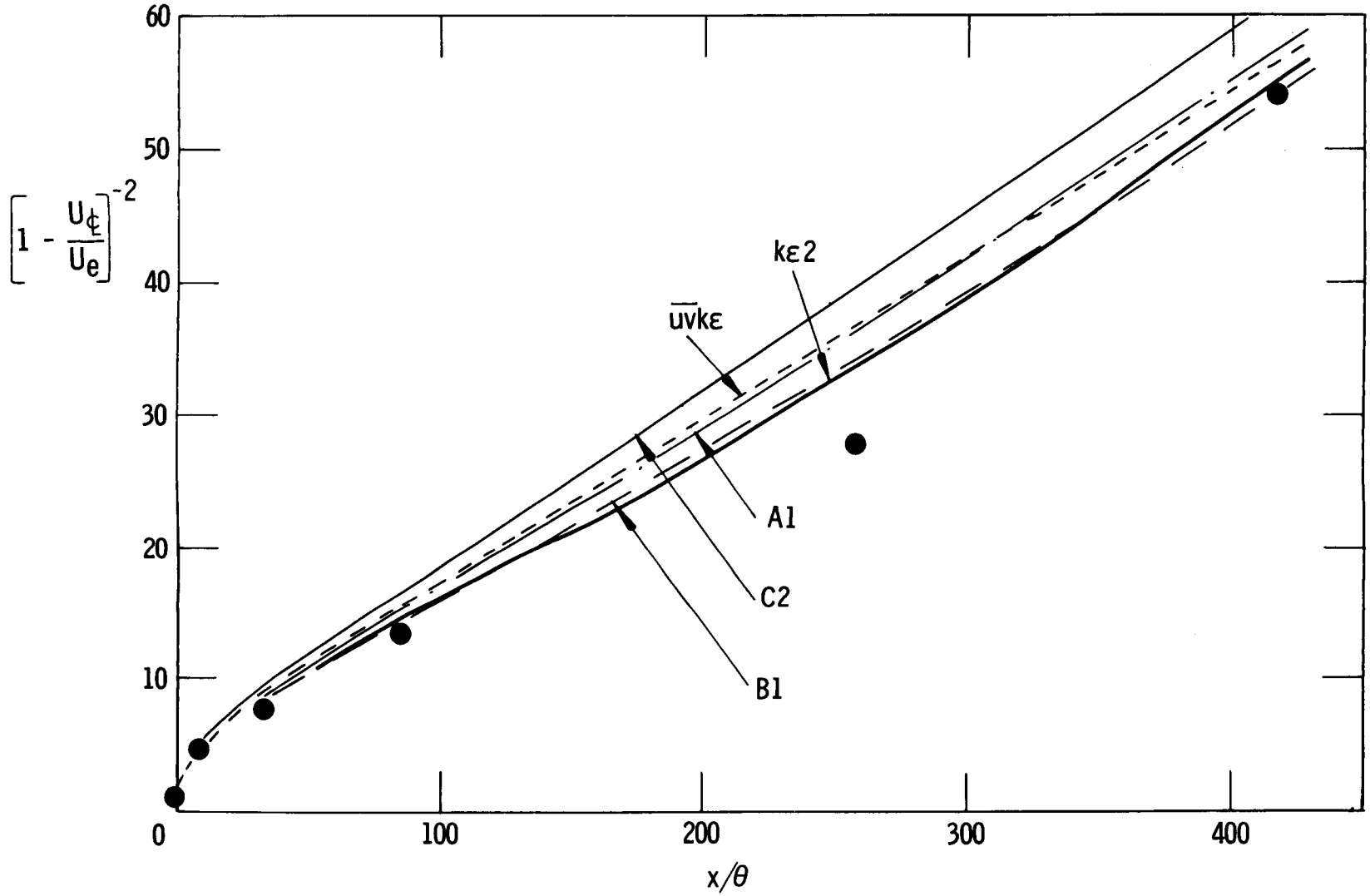

Figure 6.- Stress model predictions for case 14.

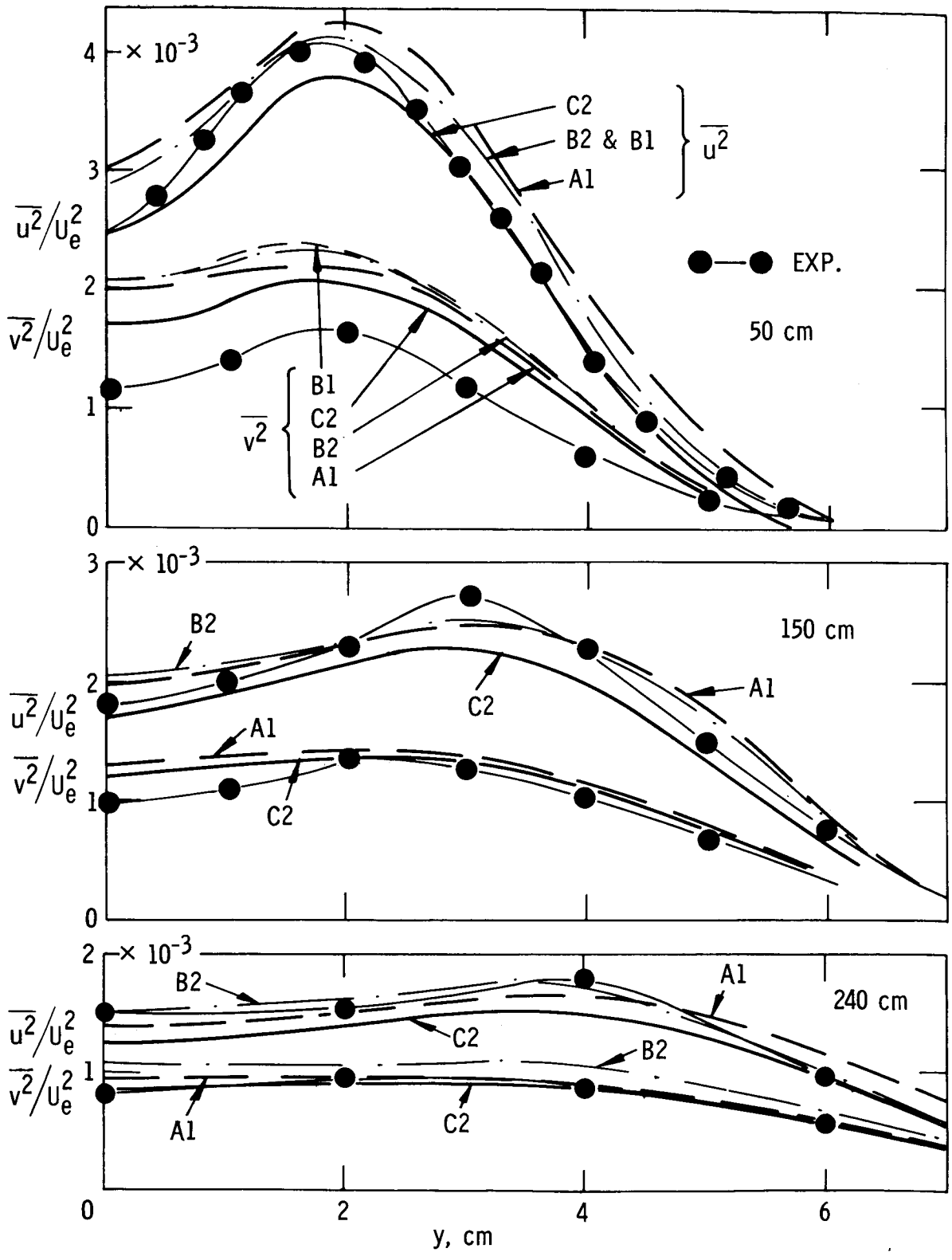

Figure 7.- Reynolds stress distributions for case 14.

DISCUSSION

D. M. Bushnell: I was wondering if you had any thoughts about the importance of the pressure-velocity correlations at compressible speeds, and how you presently handle them in your method.

D. B. Spalding: How they are handled at the present is that everything of that kind is lumped into the energy diffusion term. We simply see how well we can do by choosing the best constants, such as the effective Prandtl or Schmidt number, for turbulence diffusion, including in our review compressible or density-varying flow.

D. M. Bushnell: We have nothing to compare the diffusion model with at the compressible conditions. In other words, you are lumping a lot in there, and we are not sure how accurate the lump is.

D. B. Spalding: That is correct. All we see is the final result. We do not have enough detailed information. For incompressible flows, we can make detailed comparison; for compressible flows, we need corresponding detailed measurements and comparisons.

D. M. Bushnell: The only thing is, those terms look huge. That's my only comment.

I. E. Alber: With respect to the compressible calculations, I see that you get the results for the spreading rate for the two-dimensional mixing layer as a function of Mach number, which is quite similar to what other people have obtained; that is, there is very little variation of the spreading parameter with Mach number. However, the data, apparently the high Reynolds number data, indicate that there is a considerable increase in the spreading parameter with Mach number. Could you comment on what may be the cause of this discrepancy, and if the pressure velocity correlation effect at high speeds may come into the picture?

D. B. Spalding: I can't comment from any knowledge or any insight. I have noted the effect also, and so I wonder.

G. L. Mellor: Yes, I would like to be certain on one point that you made. Your length scale equation is a dissipation thing, which is energy to the 3/2 power over the length scale. And we know that Rotta has an equation for the transport of a velocity squared times the length scale. I think you said that you tried some of that too, and you said that it made no difference whatsoever? Is that my understanding?

D. B. Spalding: It makes little difference for the kind of flows considered in this conference, which are free turbulent flows. It is easy to explain. One can formally show that the transport equation for ϵ can be turned into the transport equation for the product of k times the length scale, except for an additional term involving the gradient across the layer of the length scale. There are many models in this family that differ only in

an additional length-scale-gradient term in the equation. That term is very small in all these flows. Flows near walls are different. There are some crucial experiments to be carried out which will enable us to distinguish between the models. But, at the practical level, the distinction between the models lies only in the different value given to the effective Prandtl number (or Schmidt) of the second turbulence quantity. There is just one good thing in favor of the ϵ models. You can have a constant value of the Schmidt number for the diffusion of this quantity, whether you are in a free turbulent flow or near a wall. All the other models, including the $k\ell$ model, require the Schmidt number to be varied, or they require something else to be done. So the $k\epsilon$ model has our favor for this quite small advantage connected with wall flows.

M. V. Morkovin: Could I ask for a comparison of your efforts and Donaldson's? In what respect are they similar and where do they depart?

B. E. Launder: Dr. Donaldson and our group at Imperial College are both developing turbulence models based on differential equations for the Reynolds stresses. We adopt in detail different approximations for the pressure-strain term; we use appreciably more elaborate closures than Dr. Donaldson. I think that he will find it necessary to use a more complicated closure when he comes to look at some of the shear flows that we have examined.

C. duP. Donaldson: We use a slightly different dissipation model. We have already started to put in more complicated pressure-strain terms that we came to from trying to use this method to study transition. This problem is similar to that of the wall region of a turbulent boundary layer. In this case, to be more complete, you do have to use mean gradients in the definition of pressure-strain and isotropy terms. I would like to make an additional comment while I've got the microphone and emphasize again what can be learned from these higher order models by setting the transport terms equal to zero and neglecting diffusion. It is really very interesting that you can see the difference between plain and axisymmetric jets and, in many cases of complicated flows with body forces or centrifugal forces, you can begin to see just where you don't want to use conventional methods.

C. E. Peters: I would like to address my question to either Professor Launder or Professor Spalding. These advanced methods depend greatly on the initial conditions, particularly in relatively weak shear flows. Your procedure of using either experimental initial conditions or an eddy viscosity which matches the initial region development only allows an after-the-fact correlation of an experiment. What is one to do in an engineering situation where the initial conditions are not well defined? Can you suggest procedures for approximately determining the initial conditions?

B. E. Launder: I would not entirely accept your assertion that our practices allow only "after-the-fact correlation." After all, if it were correct, we might expect nearly the same performance to be turned in by the various models; yet there are, in fact, large differences between predictions generated by the various models. However, I agree that when our procedures (or anyone else's for that matter) are used to predict engineering flows, insufficient experimental data will generally be available to describe the initial conditions with certainty. If the predictor has thorough acquaintance with experimental data of turbulent flows, he may well be able to assess with sufficient accuracy the initial profiles. Otherwise, the safest practice is to begin computations sufficiently far upstream for the (perhaps badly) guessed initial profiles to have negligible effect on the region of interest. For example, if one wants to predict a jet development, then computations might begin at the upstream end of the nozzle(s); or, if the flow is a wake, the calculations could start upstream of the obstacle generating the wake.

P. A. Libby: I am greatly impressed by the powers of the new methods developed by the Imperial College group and others when applied to flows with variable density, but I wonder whether we can expect the carefully selected constants in these methods to carry over without density effects to the variable density cases. My work in a simple flow shows that we must make these constants functions of the density.

B. E. Launder: Yes, it may be necessary to amend or extend our present models to provide consistently good predictions of variable density flows. The pressure-strain term would be the first term to be examined; others in the dissipation equation need to be looked at.

S. C. Lee: The turbulence kinetic energy equation consists of convection, diffusion, production, and dissipation terms. Why treat the dissipation term more favorably than the others? If we examine the figure of turbulence energy balance (shown by Professor Spalding with comparison of Bradbury's data), it appears that all terms are approximately the same order of magnitude.

B. E. Launder: In the models I have been talking about, based upon differential equations for the Reynolds stresses, the five processes of generation, dissipation, redistribution, diffusion, and convection interact to determine the local stress levels. Since we solve convective transport equations for the stress components, we may say that we account "exactly" for convection of the stresses. The generation term, too, is one that we treat without further approximation since it consists simply of the product of Reynolds stresses and mean velocity gradients. That leaves dissipation, diffusion, and redistribution to be accounted for; as you say, we solve a differential equation for the first of these but not for the other two. We could solve transport equations for the diffusion correlations as well as for the Reynolds stress and dissipation rate (Chou and a number of others have

suggested models of this kind). However, I regard this level of closure as unnecessarily elaborate since the diffusion terms are seldom decisively important in the Reynolds stress equations. I think therefore that the simpler gradient-diffusion approximation will suffice. Finally, there is the redistribution term to consider. Although this term does not appear in the turbulence energy equation (which was the equation you mentioned), it is of great influence in determining the magnitude of the individual stress components. The practice we adopt in simulating this term is, we think, suggested by the form of the exact correlation. Other practices are possible, however, and Kolovandin and Vatutin[1] describe a much more elaborate treatment involving the solution of three-dimensional elliptic differential equations. I do not believe such an approach is warranted since it seems that evaluation of the redistribution term would then absorb more computer time than all the rest of the calculation.

[1] Kolovandin, B. A.; and Vatutin, I. A.: Statistical Transfer Theory in Non-Homogeneous Turbulence. Int. J. Heat & Mass Transfer, vol. 15, no. 12, Dec. 1972, pp. 2371-2383.